# Variability of Suspended-Sediment Concentration in the Connecticut River Estuary

Author: Michael Vincent William Cuttler

Boston College

The College of Arts and Sciences

Department of Earth and Environmental Sciences

# VARIABILITY OF SUSPENDED-SEDIMENT CONCENTRATION IN THE CONNECTICUT RIVER ESTUARY

an undergraduate thesis

by

Michael Cuttler

submitted in partial fulfillment of the requirement

for Departmental Honors

May 2012

**Table of Contents**

## List of Tables and Figures

**Figure 11**: Suspended-sediment concentration, salinity and longitudinal salinity gradient transects from (a) high-slack water, (b) ebbing tide, and (c) low-slack water on November 16, 2008.

**Figure 12**: Suspended-sediment concentration, salinity and longitudinal salinity gradient transects from (a) high-slack water, (b) ebbing tide, and (c) low-slack water on June 21, 2011.

**Figure 13**: Suspended-sediment concentration, salinity and longitudinal salinity gradient transects from (a) high-slack water, (b) ebbing tide, and (c) low-slack water on July 6, 2011.

**Figure 14**: Suspended-sediment concentration, salinity and longitudinal salinity gradient transects from (a) high-slack water, (b) ebbing tide, and (c) low-slack water on November 19, 2008.

**Figure 15**: Linear regression analysis of the relationship between $L_e$ and the position of the primary turbidity maximum, $X_{TM}$ (km).

**Figure 16**: Linear regression analysis of the relationship between the position of secondary turbidity maximum, $X_{STM}$ (km) and positions of peak longitudinal-bottom salinity gradients, $X_F$ (km).

**Figure 17**: Suspended-sediment concentration, salinity and longitudinal salinity gradient transects from (a) Low water + 4.5 hours (flooding tide) and (b) high water + 3.25 hours (ebbing tide) on November 19, 2008.

**Figure 18**: Velocity transects from (a) low water + 4.5 hours (flooding tide) and (b) high water + 3.25 hours (ebbing tide) on November 19, 2008.

**Figure 19:** Vertical profiles of velocity (blue), salinity (red) and suspended-sediment concentration (green) at (a) 5.1 km, (b) 5.2 km and (c) 5.3 km upstream of the estuary mouth and (d) corresponding suspended-sediment concentration transect during ebb conditions on November 19, 2008.

**Figure 20**: Vertical profiles of velocity (blue), salinity (red) and suspended-sediment concentration (green) at (a) 5.1 km, (b) 5.2 km and (c) 5.3km upstream of the estuary mouth and (d) corresponding suspended-sediment concentration transect during flood conditions on November 19, 2008.

**Figure 21**: Vertical profiles of velocity (U) and salinity (S) from a) the Connecticut River estuary and b) the Fraser estuary (Geyer and Farmer, 1989). These profiles indicate the presence of a velocity jet associated with the pycnocline.

**Figure A1**: Discharge during the June/July 2011 study period. Discharge was measured at the USGS gage station on the Connecticut River at Thompsonville, CT.

**Figure B1**: Discharge during the November 2009 study period. Discharge was measured at the USGS gage station on the Connecticut River at Thompsonville, CT.

**Figure C1**: Discharge during the November 2008 study period. Discharge was measured at the USGS gage station on the Connecticut River at Thompsonville, CT.

## List of Symbols

| | |
|---|---|
| $\delta s$ | surface to bottom salinity difference |
| $\langle s \rangle$ | depth-averaged salinity |
| $u_s$ | net surface velocity |
| $u_f$ | mean cross-sectional velocity |
| $U_r$ | mean river velocity |
| $U_T$ | mean tidal velocity |
| $C_o$ | observed suspended-sediment concentration |
| $C_c$ | calculated suspended-sediment concentration |
| $L_e$ | length of estuary |
| $Q$ | river discharge |
| $X_{TM}$ | position of turbidity maximum |
| $X_{STM}$ | position of secondary turbidity maxima |
| $X_F$ | position of density front |
| $b_o$ | barclinic velocity |
| $g$ | gravitational acceleration |
| $\beta$ | coefficient of expansivity for salinity |
| $s_{oc}$ | oceanic salinity |
| $H$ | average estuary depth |
| $h$ | total water depth (at a station) |
| $\omega$ | angular velocity |
| $T$ | tidal period |
| $\varrho$ | water density |
| $Q_T$ | tidal discharge |
| $A$ | cross-sectional area |
| $t$ | test statistic |
| $r$ | correlation coefficient |
| $r_s$ | Spearman's rank correlation coefficient |
| $n$ | number of samples |
| $n_o$ | number of ranked pairs |
| $S_{xx}$ | sample corrected sum of squares for x-values |
| $S_{yy}$ | sample corrected sum of squares for y-values |
| $S_{xy}$ | sample covariance |

**Abstract**

Turbidity maxima are areas of elevated suspended-sediment concentration commonly found at the head of the salt intrusion in partially-mixed estuaries. The suspended-sediment distribution in the Connecticut River estuary was examined to determine where turbidity maxima exist and how they form. Field studies conducted in June/July 2011, November 2009 and November 2008 collected salinity, suspended sediment and velocity data over a range of discharge and tidal conditions in the Connecticut River estuary. Areas of enhanced suspended-sediment concentration were found to exist at all phases of the tide near the head of the salt intrusion as well as downstream of this point in deeper parts of the estuarine channel. These areas are locations where peaks in the longitudinal salinity gradient exist, suggesting the presence of a front, or zone of flow convergence. Velocity, salinity, and suspended-sediment data show that during flood conditions there is a layer of landward-flowing water in the middle of the water column that decelerates upon entering deep parts of the estuary; thus enhancing particle settling. During ebb conditions, surface waters flow faster than bottom waters, which strengthens stratification. These conditions create a nearly zero velocity layer below the pycnocline, which limits sediment resuspension and enhances settling from surface waters. The combination of processes acting throughout the tidal cycle focuses and, potentially, traps sediment in the deeper parts of the Connecticut River estuary.

**Acknowledgements**

I would like to thank the Keck Geology Consortium who funded the June/July 2011 field study through a Keck Geology Consortium summer fellowship based at Wesleyan University. I would also like to acknowledge the project coordinators from Wesleyan University, Suzanne O'Connell and Peter Patton, who helped to make the June/July 2011 field work possible.

I would like to thank David Ralston of Woods Hole Oceanographic Institution and Malcolm Scully of Old Dominion University for generously allowing me to use their unpublished data sets from field studies on the Connecticut River estuary in November 2008 and 2009, respectively.

This thesis would not have been possible without the constant advice and encouragement of my advisor, Dr. Gail Kineke. The opportunities you have provided me over the last 3 years have taught me that my passion for surfing and the coastal environment can translate into an academic passion as well.

I would like to thank Dylan Anderson for helping to keep stressful situations light, brainstorming ideas, and, most importantly, becoming one of my best friends throughout this entire year. Finally, I would like to thank my roommates and family for their never ending support and for helping me to remain positive and see the bigger picture.

## 1. Introduction

An estuary is a transitional environment located between the riverine and oceanic environments; estuaries are therefore subject to both marine and fluvial influences. Due to their location, estuaries offer naturally sheltered anchorages and waterways that are vital for shipping goods, for the development of commercially important fisheries, and for recreational use (Pinet, 2000; Trujillo and Thurman, 2011). Estuaries also act as natural filters for sediment and pollution carried by rivers to the oceans (Schubel and Kennedy, 1984). Chemical reactions in estuaries can alter the character of some mineral particles, especially clays, which can thus influence pollutant transport (Brown and Park, 1999). Circulation and deposition patterns in estuaries tends to focus sediment (contaminated or not) in specific areas. While the removal of sediment from the water column may increase marine water quality, trapping sediment in particular locations can lead to infilling of the estuarine channel and concentration of pollutants. Deposition of contaminated sediments can lead to the decline of fish populations, which alters the estuarine ecosystem and decreases the economic value of the estuary. Infilling of the estuary decreases the economic and recreational value of the estuary as navigation channels become unusable. Channel maintenance typically requires dredging, which can lead to much larger environmental issues if the deposits are contaminated with pollutants, such as heavy metals. Therefore, it is important understand sedimentation processes in estuaries in order to effectively manage and maintain estuaries in the future.

## 2. Objectives

The overall aim of this research is to assess the variability of suspended-sediment distribution in the Connecticut River estuary over a range of discharge and tidal conditions. To address this aim the following research questions were proposed:

1. Where are areas of enhanced suspended-sediment concentration found in the Connecticut River estuary?
2. What physical processes are responsible for focusing sediment in these locations?

The following investigations were completed to answer each research question:

1. Analysis of longitudinal transects of suspended-sediment concentration to identify areas of enhanced suspended-sediment concentration.
2. Comparison of positions of enhanced suspended-sediment concentration with the location of the salt wedge and peaks in the longitudinal salinity gradient.
3. Analysis of velocity transects at locations of enhanced suspended-sediment concentration to understand potential sediment trapping mechanisms.

## 3. Background

### 3.1 Estuarine Circulation and Classification

Although the definition of an estuary has evolved over time, one commonly accepted definition identifies three key characteristics of an estuary: it is a semi-enclosed coastal body of water with free connection to the ocean; it extends into the river as far as the limit of tidal influence; and sea water is measurably diluted with fresh water within the estuary (Cameron and Pritchard, 1963; Dyer, 1997).

Estuaries can be classified based on many different properties. Some of these properties include water balance, geomorphology, vertical salinity structure, and hydrodynamics (Valle-Levinson, 2010). Estuaries can also be classified by tidal range (Dyer, 1997). Microtidal, mesotidal, macrotidal, and hypertidal estuaries are characterized by tidal ranges of less than 2m, 2-4 m, 4-6 m, and greater than 6 m, respectively (Dyer, 1997).

Classification based on topography or geomorphology includes coastal plain estuaries, fjords, bar-built estuaries, and tectonic estuaries. Coastal plain estuaries, or drowned river valleys, are estuaries that formed due to Pleistocene sea level rise (Dyer, 1997). These estuaries were formerly river valleys that became inundated with seawater as sea level rose over the last 15,000 years. Coastal plain estuaries tend to be wide and shallow, such as Chesapeake Bay (Valle-Levinson, 2010). Fjords are estuaries that occur in high latitudes where glaciers greatly impact the landscape. These estuaries have deep (hundreds of meters) and narrow (tens of meters) channels that have a glacially deposited sill at the estuary mouth (Dyer, 1997). Modern examples of fjords can be found in Puget Sound as well as in Greenland and Alaksa (Valle-Levinson, 2010). Bar-built estuaries were originally embayments that became semi-enclosed due to the creation of a sand bar or spit by littoral drift. These sand bars and spits may be

extensions of nearby headlands, which lead to a single connection between the estuary and the sea, or may be barrier islands, which allow for two or more inlets to the sea. Bar-built estuaries are common in North Carolina, Florida and northern Mexico (Valle-Levinson, 2010). Tectonic estuaries are formed by tectonic events, such as earthquakes and faulting, that create basins that adjacent water bodies can occupy. San Francisco Bay is an example of a tectonic estuary (Valle-Levinson, 2010).

Another classification of estuaries is based on salinity structure. This classification considers the competition between buoyancy forcing from river discharge and mixing forces from tides (Valle-Levinson, 2010). A salt wedge estuary is created when the river discharge is large and the tidal forcing is weak (Figure 1a; Brown and Park, 1999; Valle-Levinson, 2010). In these estuaries, buoyant fresh water flows seaward on top of the denser salt-water wedge. Through a process known as entrainment, shearing forces on the halocline (the interface between fresh and salt water) generate turbulence, which causes salt water to be transported seaward with the surface flow. The lost salt water is replaced by a residual landward flow of seawater along the estuary bottom to maintain a salt-balance (i.e. the estuary is not freshening over time). This two-layered flow pattern is known as gravitational or estuarine circulation. Along the estuary, salinity in the surface and bottom layers will be almost constant except for zones at the head of the wedge where the halocline meets the bottom, and at zones downstream where the halocline meets the surface. The position of the salt wedge varies with river discharge and tidal phase (Dyer, 1997).

Partially-mixed estuaries occur when discharge is small compared with the tidal prism (Figure 1b; Brown and Park, 1999; Dyer, 1997; Valle-Levinson, 2010). Increased tidal forcing enhances friction between the landward-flowing seawater and the bed, generating turbulent

eddies. The turbulent eddies are effective at vertically mixing salt water upwards and fresh water downwards. The increase in salt-water removal from bottom waters strengthens the estuarine circulation as a greater volume of seawater is required to flow landward to maintain the overall salt balance of the estuary. At some depth in the water column, the mean flow is equal to zero, which is known as the level of no motion (Dyer, 1997). When the level of no motion intersects the bed there is a convergence of bottom flows; this convergence point is called the null point. In partially-mixed estuaries, a longitudinal salinity gradient is present in both the surface and bottom waters: salinity increases seaward in surface waters and salinity decreases landward in bottom waters (Dyer, 1997).

Well-mixed estuaries occur when tidal range is large relative to water depth and river discharge (Figure 1c; Brown and Park, 1999; Dyer, 1997). The turbulence generated in these estuaries is sufficient to completely mix the water column and make the estuary vertically homogenous. The estuarine circulation tends to break down because inflowing salt water is rapidly mixed throughout the water column. Well-mixed estuaries can experience laterally inhomogenous or laterally homogenous flow circulation. Laterally inhomogenous flow occurs in estuaries that are wide enough for Coriolis and centrifugal forces to affect flows. In these estuaries flow is landward on one side and seaward on the other. In laterally homogenous flows, lateral shear is strong enough to create laterally homogenous conditions. This allows salinity to increase evenly seaward and leads to mean seaward flow, which removes salt from the estuary (Dyer, 1997).

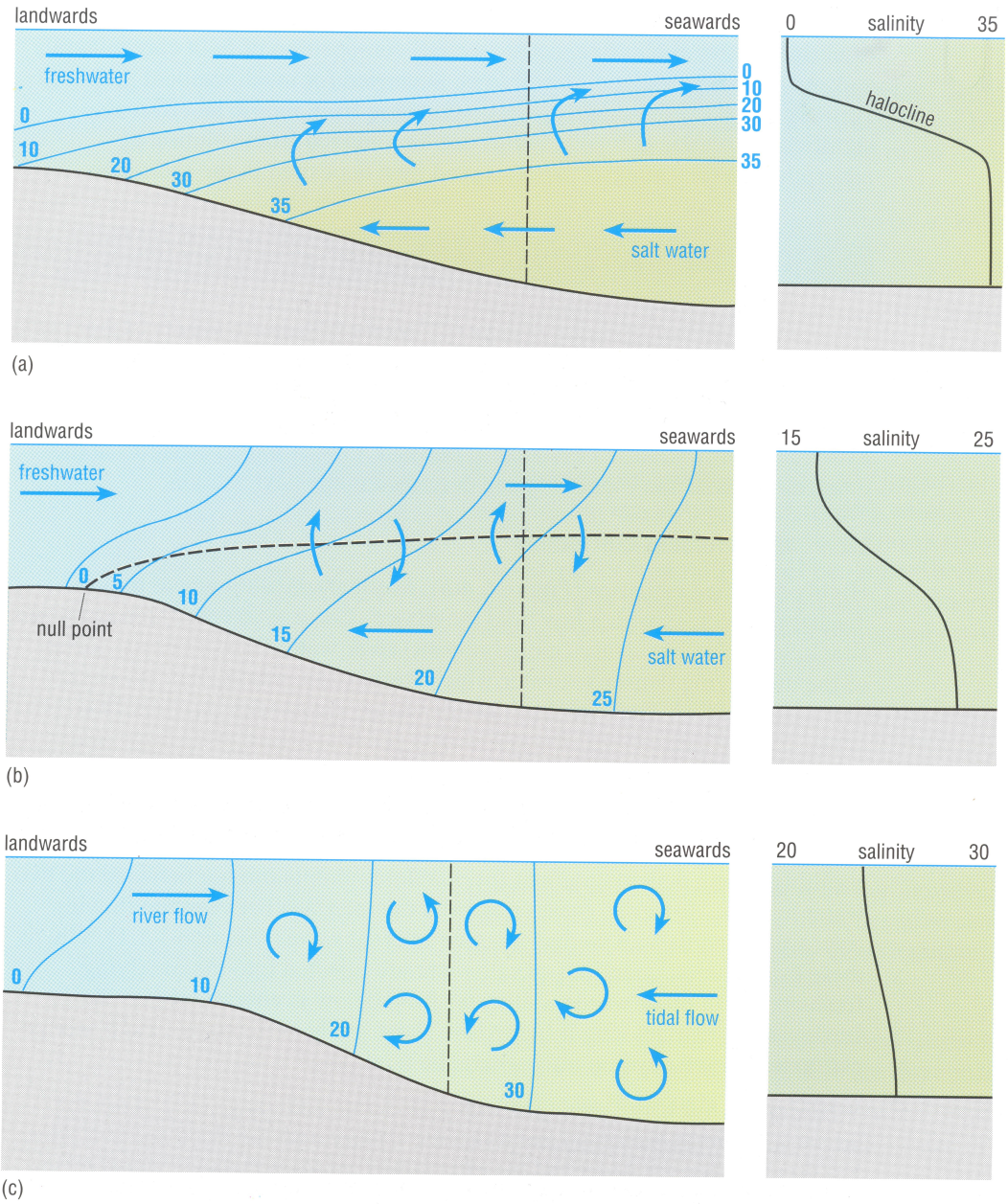


Figure 1: Representations of water circulation and salinity profile in a (a) salt wedge, (b) partially-mixed, and (c) well-mixed estuary. Vertical dashed lines show position of salinity profile. (Brown and Park, 1999).

Estuaries can also be classified according to their hydrodynamics. Hansen and Rattray (1966) developed a form of this classification based on stratification and circulation parameters. The stratification parameter, $\frac{\delta s}{<s>}$, is the surface to bottom salinity difference divided by the

depth-averaged salinity. The circulation parameter, $\frac{u_s}{u_f}$, is the ratio of the net surface velocity to the mean cross-sectional velocity (Hansen and Rattray, 1966; Dyer, 1997). This ratio classifies estuaries into four categories. Type 1 estuaries, with circulation parameters of 1.5 and stratification ranging from $10^{-2}$ to $10^{-1}$, exhibit net seawards flow at all depths and upstream salt transport is accomplished by diffusion. Type 2 estuaries, with circulation parameters of 10 and stratification ranging from $10^{-2}$ to $10^{-1}$, have flow reversal with depth and correspond to the partially-mixed estuary. In Type 3 estuaries, where the circulation parameter is between $10^3$ and $10^4$ and stratification ranges from $10^{-2}$ to 1, salt transport is primarily advective. Type 4 estuaries, with circulation parameters of 1.5 and stratification greater than 1, exhibit intense stratification, like the salt-wedge estuary (Hansen and Rattray, 1966; Dyer, 1997).

Hansen and Rattray's classification system is a diagnostic approach, meaning that it classifies an estuary based on an observed set of conditions. A more prognostic approach that allows one to predict the estuarine classification based on two forcing variables was established by Geyer (2010). These two 'master variables' are $U_R$, mean river velocity, and $U_T$, mean tidal velocity. Classifying estuaries in this way allows for better comparison because estuaries that plot in similar parameter space are expected to experience similar dynamics (Geyer, 2010).

### 3.2 Estuarine Sediments and the Estuarine Turbidity Maximum

Estuarine sediments are dominated by fine-grained material because estuaries are usually located far from the source of sediments. These fine-grained sediments are predominantly silts, clays and some organic material. These particles tend to be cohesive, which is mainly due to the clay fraction (Partheniades, 2009). The surfaces of clay particles have a negative charge, which causes repulsion between particles in fresh water. However, in seawater, cations neutralize the negative charge and allow these clay particles to be brought close together via turbulence and

Brownian motion (Partheniades, 2009). When the particles are sufficiently close together they experience van der Waals forces, that bind them together in a process called flocculation (Brown and Park, 1999). These sediment bundles, known as "flocs," have a higher settling velocity than individual particles, leading to enhanced deposition.

A distinguishable feature in most partially-mixed estuaries is a turbidity maximum (TM), which is an area with higher suspended-sediment concentration than any other part of the estuary (Brown and Park, 1999). Concentrations within the TM can be 100 to 200 mg/L in mesotidal estuaries and up to $10^3$ to $10^4$ mg/L in higher tidal range areas (Brown and Park, 1999; Dyer, 1997). The TM is generally associated with the maximum landward extent of the salt intrusion (Figure 2; Brown and Park, 1999; Dyer, 1997). A TM is generated in the vicinity of the head of the salt intrusion because suspended sediment is transported here by both fresh and saline waters. Sediment is also concentrated here by enhanced particle settling from flocculation and increased stratification. (Geyer, 1993; Dyer, 1997). The position of the TM is related to the river discharge, with the TM moving seawards with increasing discharge (Uncles and Stephens, 1989). TM position and suspended-sediment concentration also vary with the tidal cycle. At high-slack water, the TM is up-estuary and concentrations are relatively low due to settling. During ebb tide, the TM migrates down estuary and suspended-sediment concentrations tend to increase as sediment is re-suspended or eroded from the bed. Settling and lower concentrations again occur at low-slack water. The cycle repeats at the onset of the flood tide with renewed resuspenion or erosion of sediment from the bed (Dyer, 1997).

Secondary TMs, or regions of enhanced turbidity seaward of the head of the salt intrusion, can also form in estuaries. The formation of secondary TMs results from a combination of multiple processes, including: convergence of bottom residual flow, tidal

asymmetry, inhibition of turbulent diffusion by stratification, and bottom resuspension (Lin and Kuo, 2001).

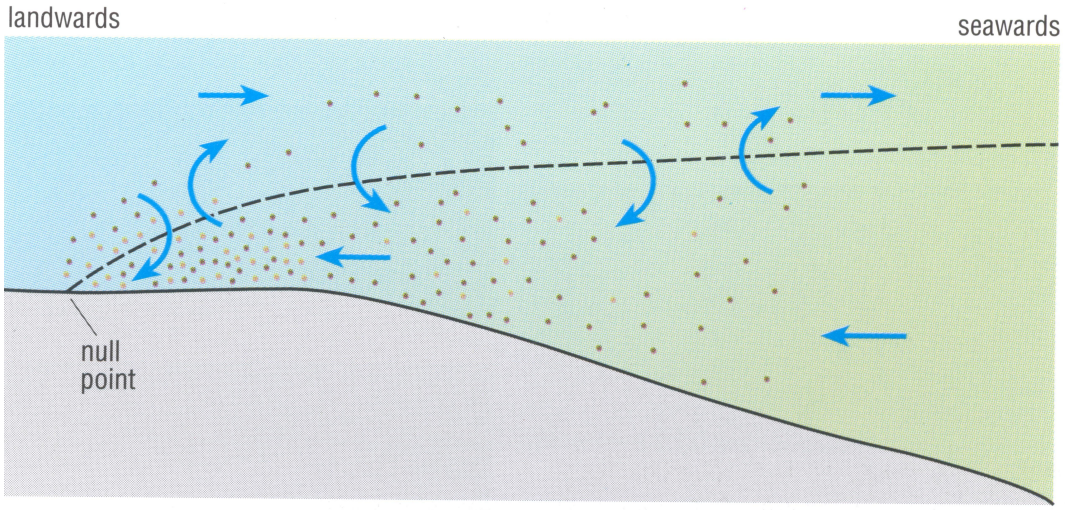


Figure 2: Representation of a turbidity maximum in a partially-mixed estuary. Horizontal blue arrows depict river discharge or tidal inflow; vertical blue arrows represent turbulent mixing along the halocline (dashed line). Suspended sediments are represented by brown dots (Brown and Park, 1999).

### 3.3 Estuarine Fronts

Fronts, or zones of flow convergence, are regions of intensified horizontal gradients that may play an important role in determining areas of fine-sediment accumulation (Kineke et al., 2001). Estuarine fronts develop due to the density differences between converging fresh and saline waters.

Bottom fronts will form seaward of constrictions or sills, due to convergence of flow on the downstream side of the constriction or sill during ebbing tide conditions (Kineke et al., 2000). Fronts may also occur in deeper or wider sections of the estuary (Largier, 1992). Kineke et al. (2000) suggest three factors that contribute to the formation of fronts: stratification, an adverse pressure gradient and a baroclinic effect. In order to consider the factors, Geyer (pers. comm.) proposes three equations that, together, describe theoretical conditions for density-dependent frontogenesis. The first equation represents stratification:

$$1 \leq \frac{U_T}{\sqrt{\frac{\Delta\rho}{\rho} gh}} < 2 \quad (\mathbf{1})$$

where $U_T$ is defined as above, h is total water depth, g is gravitational acceleration, and ϱ is water density. The second equation represents an adverse pressure gradient:

$$\frac{\frac{\delta U_T}{\delta x}}{\omega} > 1 \quad (\mathbf{2})$$

where $\frac{\delta U_T}{\delta x}$ is the tidal velocity gradient and ω is angular velocity equal to $\frac{2\pi}{T}$. Finally, the third equation represents a baroclinic pressure gradient:

$$\frac{\frac{g}{\rho}\frac{\delta\rho}{\delta x}h}{\omega U_T} > 0.2 \quad (\mathbf{3})$$

where $\frac{\delta\rho}{\delta x}$ is the pressure gradient and all other terms are defined above. Fronts can act as effective sediment traps for fine-grained, suspended sediment due to the convergence of horizontal bottom flow and enhanced stratification at the head of the front (Kineke et al., 2001). Therefore, understanding where frontogenesis, or front formation, occurs in an estuary can help to predict where areas of enhanced suspended-sediment concentration may be found.

**3.4 The Connecticut River Estuary**

The Connecticut River, which flows 650 km from its headwaters in Canada to its mouth in the Long Island Sound and drains an area of 29,000 $km^2$, is the third largest river on the east coast of the United States and the largest river in New England (Figure 3; Horne and Patton, 1989; Woodruff, in revision). Throughout most of Massachusetts and northern Connecticut, the river meanders across a broad flood plain cut into the glacial deposits of the Hartford Basin. Near Middletown, Connecticut, the river leaves the Hartford Basin and flows through the metamorphic highlands of eastern Connecticut. Near Essex, Connecticut, approximately 11 km

upstream of the mouth, the river flows into a low-relief coastal plain environment and then empties into the Long Island Sound (Figure 3; Horne and Patton, 1989).

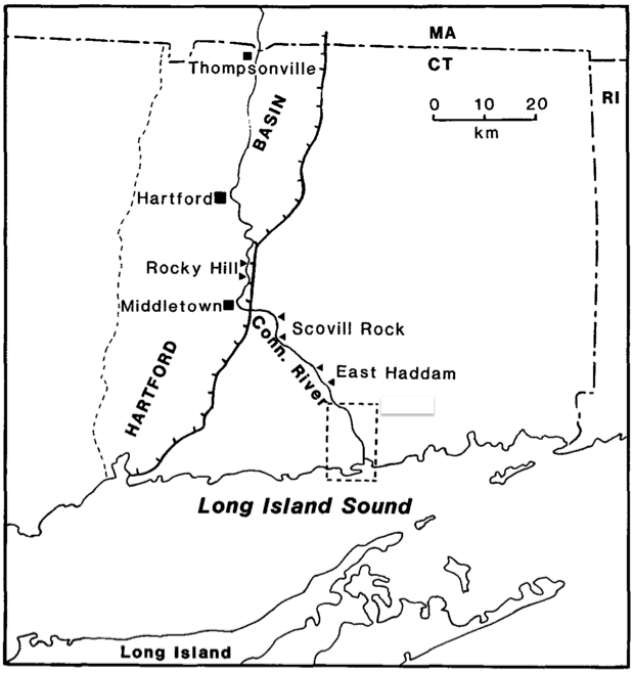


Figure 3: Location of the Lower Connecticut River in Connecticut, from Horne and Patton (1989).

Although the Long Island Sound is itself an estuary, it can be considered a marginal sea or low-energy continental shelf with respect to processes within the Connecticut River estuary because tidal mixing along the Connecticut shoreline eliminates the halocline (Gordon, 1980). Salinity in Long Island Sound is approximately 26 to 28 psu (Horne and Patton, 1989). The Connecticut River has a mean annual discharge of approximately 500 $m^3/s$ and experiences a mean tidal range of approximately 1.1 m (Woodruff, in revision). Depending on season and phase of the spring-neap tidal cycle, the Connecticut River estuary ranges from a partially-mixed estuary to a salt wedge (Garvine, 1975; Horne and Patton 1989).

While the tidal influence reaches approximately 100 km upstream, the landward extent of the salt intrusion is approximately 15 km in length (Horne and Patton, 1989). The estuary can be divided into two sections, separated by Amtrak Railway Bridge at approximately 5.5 km

upstream from the mouth. In the upper estuary, channel sinuosity is determined by bedrock headlands and the thalweg meanders around regularly spaced bars. The bed of the thalweg has ripples and megaripples that are reassembled each tidal cycle. The alternating bars typically have southward migrating dunes. The upper estuary is deeper than the lower estuary with a mean depth of 8 m (Horne and Patton, 1989). The lower estuary is funnel shaped and widens greatly as it leaves the upper estuary. This area of the estuary has many large coves fringed by salt marsh. Shoal margins flanking the main channel have dunes and ripples or megaripples that migrate southward. The mouth of the estuary has been modified with a jetty and breakwater for navigation purposes.

Previous studies of the suspended-sediment dynamics in the Connecticut River estuary were conducted by Lemieux (1983), Massad (1984) and Bohlen (1996). Under low flow conditions, the estuary is partially-mixed and two-layer flow exists (Lemieux, 1983). During these conditions, net transport of suspended sediment is landward. During freshet conditions, salt water is completely expelled from the estuary and sediment inflow at the head essentially equals sediment outflow at the mouth. Lemieux (1983) has also shown that the background concentration in the estuary is approximately 12 mg/L and that near-bed suspended-sediment concentration varies over half-tidal cycles, suggesting resuspension by tidal currents. Peak flood transport rates occur shortly after low-slack water, whereas peak ebb transport occurs towards the later stages of the ebb tide (Massad, 1984). A TM has been observed to form on the flooding or ebbing tides, with areas of heightened suspended-sediment concentration occurring in deeper parts of the estuary at slack water (Bohlen, 1996; Massad, 1984).

## 4. Methods

### 4.1 June/July 2011

*4.1.1 Field Methods*

The June/July 2011 field study was conducted from June 12, 2011 to July 6, 2011 as part of a Keck Geology Consortium Summer Fellowship based at Wesleyan University. The study area was an approximately 11 km reach of the Connecticut River estuary and consisted of 17 sampling stations (Figure 4).

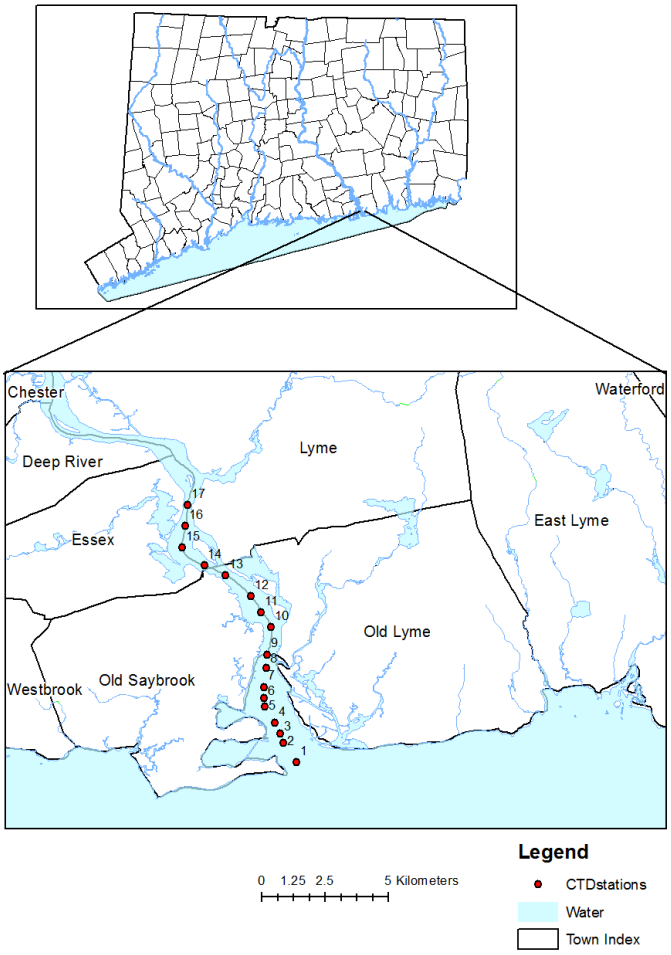


Figure 4: General study area in the Connecticut River estuary. Red circles indicate CTD and water sample stations for June/July 2011. Sampling for November 2008 and 2009 was not carried out at repeated stations, but between specific points, within this study area, on different days. Station 8 is the location of the Amtrak Railroad Bridge.

Sampling occurred on four days during the study period: June 16, June 21, June 27 and July 6. On each sampling day, longitudinal-hydrographic surveys were conducted at high slack water, low slack water and the corresponding ebbing or flooding tide. Each hydrographic survey required approximately 1.5 hours and began at the mouth of the estuary and worked landwards until the presence of salt was no longer detected in the water column. At each station, an RBR XR-620 CTD was used to measure conductivity, temperature and density of the water column. A D&A Instruments optical backscatterance sensor (OBS) attached to the CTD measured suspended-sediment concentration. One cast, which consisted of lowering and raising the instrument package through the water column, was conducted at each station during a transect and required between 30 and 60 seconds to complete, depending on water depth.

Two different RBR-OBS configurations were used throughout the study period. The initial configuration was used on June 16 and June 21 and consisted of attaching the RBR-OBS to a steel frame (Figure 5a). The face of the OBS and the RBR sensors were approximately 15 cm from the base of the frame. A 10 lb weight was attached to the base to minimize the drag on the instrument package while it was being lowered through the water column.

The second RBR-OBS configuration, used on June 27 and July 6, consisted of attaching the RBR-OBS to a vertical frame that also had a 1.58 L Niskin bottle attached to it (Figure 5b). The Niskin bottle was triggered when the 'foot' of the package hit the bottom, collecting a bottom water sample. The OBS face and the RBR sensors were again mounted at approximately 15 cm above the bottom when the 'foot' was triggered.

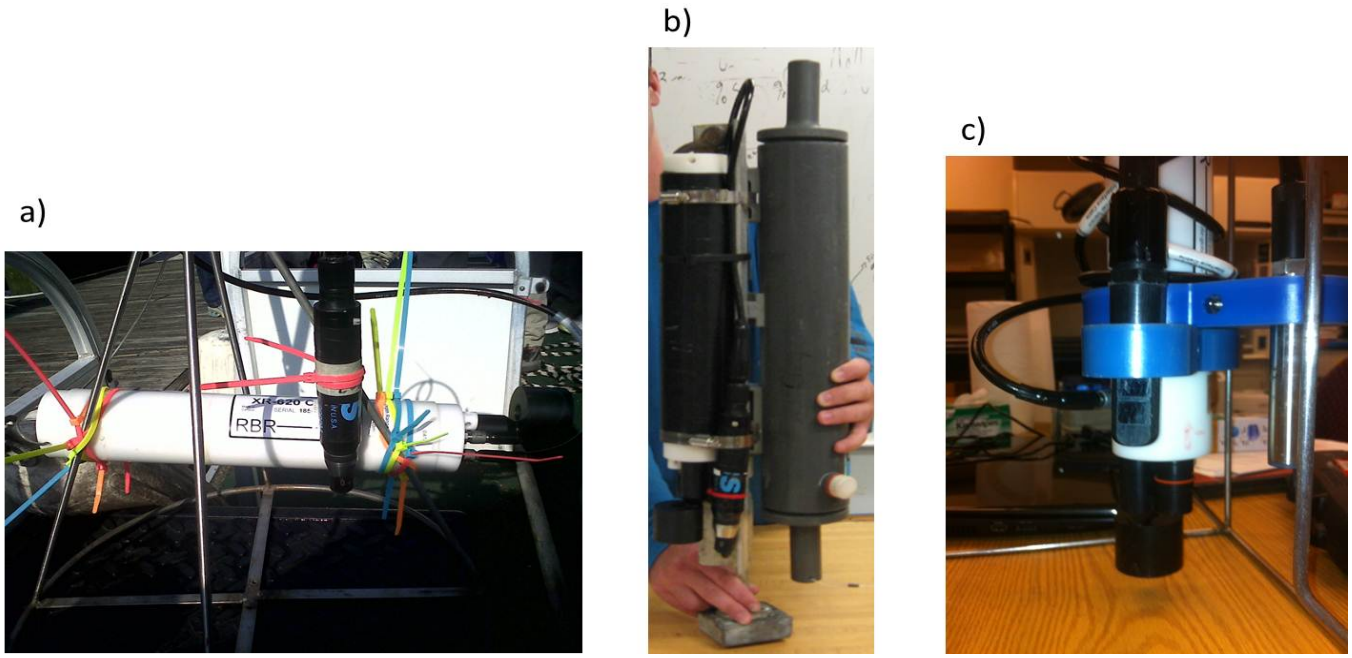


Figure 5: Image of the RBR-OBS instrument package used on: (a) June 16 and June 21, 2011, (b) June 27, 2011 and July 6, 2011, and (c) November 18, 2009.

*4.1.2 Suspended-Sediment Concentration*

In addition to hydrographic surveys, water samples were collected at each station in 500 mL Nalgene bottles using a weighted hose with 0.5 m markings and a pump run on the vessel. When collecting water samples, the hose was lowered until the weight hit the bottom, water was then pumped through the hose for 30 seconds and then Nalgene bottle was filled with water from that depth. At most stations, samples were collected every other meter from the bottom to 1 meter below the surface. Surface samples were collected by dipping a Nalgene bottle over the side of the boat.

A vacuum pump filtration system was used to filter the contents of all of the Nalgene bottles. Water samples were filtered through 1 micrometer Millipore glass filters except for the bottom water samples collected using the second RBR-OBS package, which were filtered through 0.45 micrometer Millipore microcellulose filters. After filtering, the filters were allowed

to air dry for approximately three days and then were re-weighed. Suspended-sediment concentration was calculated using the follow equation:

$$\text{SSC}\left(\frac{\text{mg}}{\text{L}}\right) = \frac{(\text{post weight (g)} - \text{pre weight (g)}) * 1000}{\frac{\text{volume filtered (mL)}}{1000}} \quad (\mathbf{4})$$

The water samples collected using the second RBR-OBS package were used for an initial calibration of the OBS (Figure 6a). Although a total of 80 samples were collected, 19 were excluded from the calibration due to unrealistic OBS readings at the bottom, likely due to resuspension when the package hit the bottom. A linear regression analysis yielded the following relationship:

$$\text{SSC}\left(\frac{\text{mg}}{\text{L}}\right) = 47 * \text{OBS} + 8 \quad (\mathbf{5})$$

The initial calibration had a sample size, n, of 61 and a correlation coefficient, r, of 0.7. A hypothesis test was conducted to determine the statistical significance of the correlation for this case (Mendenhall et al., 2009); the test statistic, t, was calculated as:

$$t = r\sqrt{\frac{n-2}{1-r^2}} \quad (\mathbf{6})$$

where r is the correlation coefficient (Mendenhall, 2009). With a t-score of 7.53 and n = 61, this relationship is significant at the 99% level of statistical significance. However, despite the significance, ten more points were excluded due to high OBS readings that were suspected to be caused by interference at the surface, i.e. the OBS can be affected by a reflective surface or direct sunlight (D&A Intstrument Co., 1991). A second linear regression analysis determined the new relationship to be:

$$\text{SSC (mg/L)} = 60 * \text{OBS} + 11 \quad (\mathbf{7})$$

With a t-score of 15.86 and n = 51, this relationship is also significant at the 99% level of statistical significance (Figure 6b).

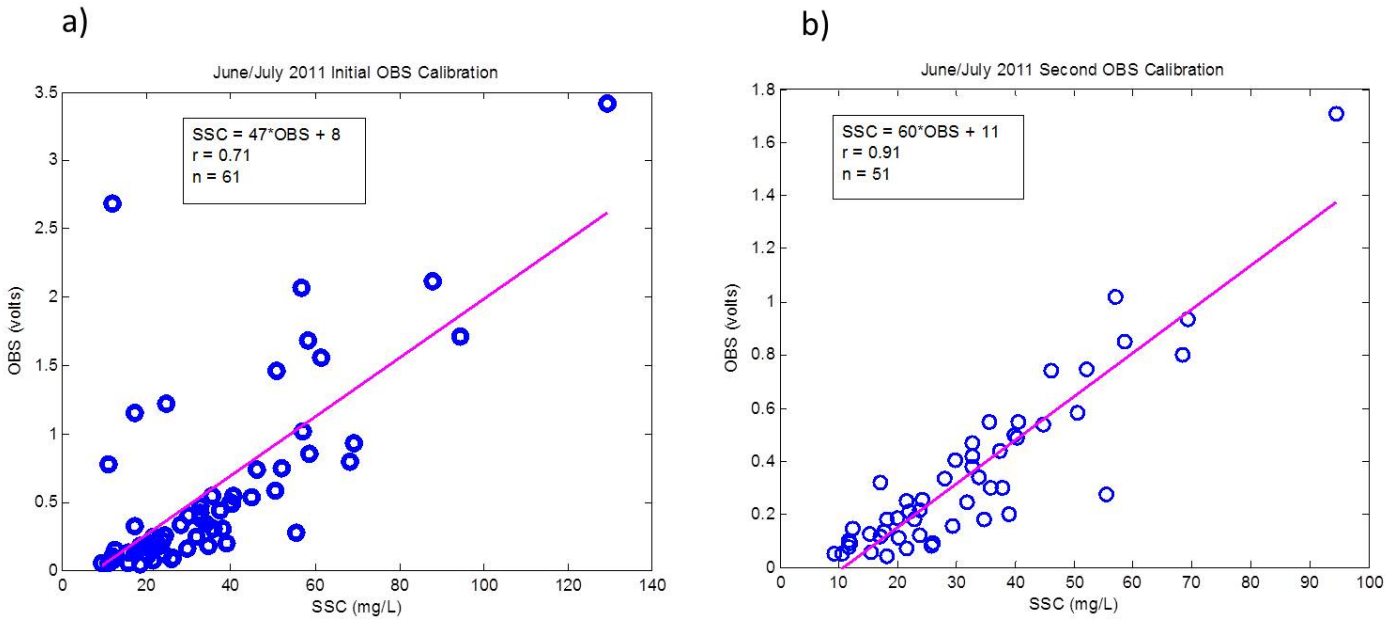


Figure 6: (a) Initial calibration and (b) second calibration of the OBS using bottom water samples collected on June 27 and July 6 2011.

The root mean square (RMS) of the data was calculated using Equation 8:

$$\mathrm{RMS} = \sqrt{\frac{1}{n}\sum(C_o - C_c)^2} \qquad (8)$$

where $C_o$ is the observed suspended-sediment concentration and $C_c$ is the suspended-sediment concentration calculated using Equation 7. The RMS for Equation 5 and Equation 7 were calculated to be 12 and 8 mg/L, respectively. Equation 7 was then applied to every cast in the data set in order to calculate suspended-sediment concentration for the study period.

*4.1.3 Averaging and Contouring*

Data were processed and edited using the numerical processing package MATLAB. RBR data were imported into MATLAB and separated into individual casts. Each cast was bin-averaged, with a bin size of 0.2 m, and then organized into longitudinal transects. The density of

water is a function of temperature and salinity. In an estuary, salinity dominates over temperature in determining water density (Ralston et al., 2010); therefore, salinity was presented as representative of the density structure of the estuary. Salinity and suspended-sediment concentration were contoured using the contour function in MATLAB. Salinity was contoured to specific levels: 0, 2, 5, 10, 15, 20, 25, and 30 psu. Suspended-sediment concentration was also contoured to specific values: 0, 10, 20, 30, 40, 50, 60, 70, 80, 90, 100, 150, 200 and 250 mg/L.

**4.2. November 2009**

*4.2.1 Field Methods*

A research cruise was conducted from November 16, 2009 to November 19, 2009 in an approximately 3 km reach of the Connecticut River estuary (Figure 4, stations 6-11). Hydrographic surveys were conducted rapidly during ebbing or flooding tides in order to try to observe the formation of bottom fronts and required approximately 30 min to complete. An RBR XR-620 CTD was used to measure vertical profiles of conductivity, temperature, and density. A D&A Instruments OBS was attached to the RBR in order to measure suspended-sediment concentration. The OBS and conductivity sensors were 16 cm and 5 cm, respectively, from the bed when the package reached the bottom (Figure 5c).

Hydrographic data were also collected outside of the estuary mouth, however, these data were not included because this study focuses on the estuarine processes occurring between the mouth and the furthest landward point of seawater intrusion.

*4.2.2 Suspended-Sediment Concentration*

On November 18, 2009, surface and bottom water samples were collected in order to calibrate the OBS. Surface samples were collected by dipping a Nalgene bottle over the side of the boat. Samples were collected via the Niskin bottle that was part of the instrument package.

These water samples were filtered and weighed to calculate suspended-sediment concentration in mg/L (Equation 4). These concentrations were then used to calibrate the OBS (Figure 7).

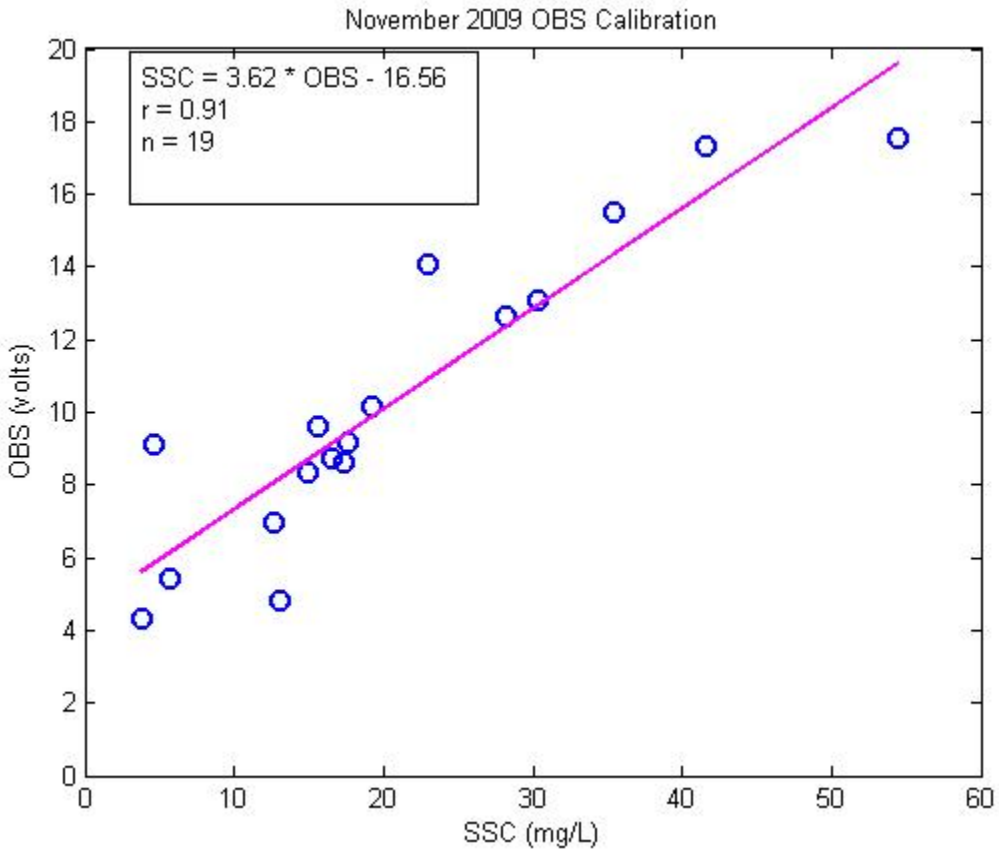


Figure 7: Calibration of the OBS from water samples collected on November 18, 2009. This calibration was used to calculated suspended-sediment concentrations for each cast in the November 2009 data set.

A linear regression analysis yielded the following equation:

$$\mathrm{SSC} = 4 \ * \mathrm{OBS} - 17 \qquad (\mathbf{9})$$

With a t-score of 9.26 and n = 19, this relationship is significant at the 99% level of statistical significance. The RMS of the data was determined to be 7 mg/L (Equation 8). Equation 9 was then applied to every cast in the data set in order to calculate suspended-sediment concentration for the study period.

*4.2.3 Averaging and Contouring*

The RBR data were processed and edited using MATLAB. The data was separated into individual casts, which were bin-averaged using a bin size of 0.2 m. The casts were organized into longitudinal transects and then salinity and suspended-sediment concentration were contoured using the contour functions in MATLAB, as described in section 4.1.3.

**4.3 November 2008**

*4.3.1 Field Methods*

A research cruise was conducted from November 16, 2008 to November 20, 2008 in an approximately 11 km reach of the Connecticut River estuary (Figure 4). Two ships, the *Tioga* and the *Mytilus* (Woods Hole Oceanographic Institution), were used to conduct longitudinal surveys of velocity, salinity and suspended-sediment concentration. The *Tioga* recorded velocity measurements, using an Acoustic Doppler Curent Profiler (ADCP), specifically between 4.5 and 5.3 km, while the *Mytilus* collected CTD and suspended-sediment profiles over the entire study area and also focused in on the *Tioga* area.

Two different RBR XR-620 CTDs were used to measure conductivity, temperature, depth, salinity and density. One of the RBRs was an internally recording instrument with a pressure sensor, the other recorded in real-time but had no pressure sensor. A D&A Instruments OBS was attached to both RBRs to measure suspended-sediment concentration. The OBS was positioned 25 cm and 2 cm above the conductivity cell for the real-time and internally-recording RBRs, respectively.

Sampling methods varied throughout the study period in order to measure the physical structure of the entire estuary and to analyze specific areas where frontogenesis was likely occurring. *Mytilus* and *Tioga* sampling methods are summarized in Table 1 and Table 2, respectively.

*4.3.2 Suspended-Sediment Concentration*

No water samples were collected during this study period to calibrate the OBS; therefore, an approximate relationship between OBS output, in nephelometric turbidity units (NTU), and suspended-sediment concentration, in g/L, was used to estimate suspended-sediment concentration (D&A Intstrument Co., 1991).

$$4{,}000 \text{ NTU} = 5\frac{\text{g}}{\text{L}} \qquad (\mathbf{10})$$

This conversion was used to estimate suspended-sediment concentration for the entire study period.

*4.3.3 Averaging and Contouring*

The RBR data were processed and edited using MATLAB. The data were separated into individual casts and then bin-averaged with a bin size of 0.1 m. Individual casts were then organized into transects and salinity and suspended-sediment concentration were contoured as discussed in section 4.1.3.

| Date | Number of Transects | Time per transect (min) | Sampling Direction | Location (km) |
|---|---|---|---|---|
| Nov. 16, 2008 | 4 | 60 | Seaward | Mouth – 11 |
| Nov. 17, 2008 | 5 | 45 | Seaward | Mouth – 11 |
| Nov. 18, 2008 | 13 | 30 – 45 | Landward | Mouth – 11 (flood)<br>4 -6 (ebb) |
| Nov. 19, 2008 | 13 | 30 | Landward | 4 – 8 |
| Nov. 20, 2008 | 16 | 30 | Landward | 4 – 8 |

Table 1: Summary of sampling methods used aboard the *Mytilus* during November 2008. Distances are measured upstream from the mouth.

| Date | Number of Transects | Time per transect (min) | Sampling Direction | Location (km) |
|---|---|---|---|---|
| Nov. 16, 2008 | 2 | 45 | Seaward | Mouth – 11 |
| Nov. 17, 2008 | 1 | 60 | Seaward | Mouth – 11 |
| Nov. 18, 2008 | 1 | 60 | Landward | Mouth – 6 |
| Nov. 19, 2008 | 13 | 20 | Landward | 4.4 – 5.4 |
| Nov. 20, 2008 | 16 | 20 | landward | 4.4 – 5.4 |

Table 2: Summary of sampling methods used aboard the *Tioga* during November 2008. Distances are measured upstream from the mouth.

## 5. Results

### 5.1 Estuarine Classification and Length of Estuary

The discharge and tidal conditions observed during the field experiments are summarized in Tables 3-5. The greatest variation in discharge, measured at Thompsonville, CT, occurred during the June/July 2011 study, when discharge varied from 334 to 852 $m^3/s$ (Figure A1). While 334 $m^3/s$ is a typical summer discharge for the Connecticut River, 852 $m^3/s$ is much higher than normal and is typically observed in the spring or fall (Lemieux, 1983). During the November 2009 and November 2008 study periods, discharge varied by less than 150 $m^3/s$, from approximately 650 to 800 $m^3/s$ (Figures B1 and C1).

The greatest variation in tidal range, measured at Old Lyme, CT, occurred during the November 2008 study where tidal range varied by 0.35 m over the five sampling days (Table 3). During the June/July 2011 study and the November 2009 study, tidal range varied by 0.25 m and 0.21 m, respectively, over the different sampling days (Table 4; Table 5). Combined, all three studies cover a range of spring and neap tidal conditions, with maximum tidal range occurring during November 2008 (Table 5) and minimum tidal range occurring during June/July 2011 (Table 3). With a tidal range of less than 2 m on each study day, the Connecticut River estuary is a microtidal estuary (Dyer, 1997).

| Date | Discharge ($m^3/s$) | Tidal Range (m) | Tidal Phase | $L_e$ (km) |
|---|---|---|---|---|
| Nov. 16, 2008 | 675 | 1.43 | Ebbing | 9.05 |
| | | | Ebbing | 7.67 |
| | | | Ebbing | 6.02 |
| | | | Ebbing | 4.51 |
| Nov. 17, 2008 | 720 | 1.14 | Flooding | 5.44 |
| | | | Flooding | 6.65 |
| | | | Flooding | 8.04 |
| | | | Flooding | 9.50 |
| | | | High-slack water | 10.06 |
| Nov. 18, 2008 | 683 | 1.21 | Flooding | 6.01 |
| | | | Flooding | 7.80 |
| | | | Flooding | 8.78 |
| | | | Flooding | Not sampled |
| | | | Flooding | 9.99 |
| | | | Flooding | Not sampled |
| | | | High-slack water | 10.52 |
| | | | High-slack water | Not sampled |
| | | | Ebbing | Not sampled |
| | | | Ebbing | Not sampled |
| | | | Ebbing | Not sampled |
| Nov. 18, 2008 | 683 | 1.21 | Ebbing | 8.00 |
| | | | Ebbing | 7.80 |
| Nov. 19, 2008 | 652 | 1.08 | Flooding | Not sampled |
| | | | Flooding | 7.92 |
| | | | Flooding | Not sampled |
| | | | Flooding | Not sampled |
| | | | Flooding | Not sampled |
| | | | Flooding | Not sampled |
| | | | Flooding | |
| | | | High-slack water | Not sampled |
| | | | Ebbing | Not sampled |
| | | | Ebbing | Not sampled |
| | | | Ebbing | Not sampled |
| | | | Ebbing | Not sampled |
| | | | Ebbing | Not sampled |

Table 3: Summary of discharge and tidal conditions during November 2008.

| Date | Discharge ($m^3/s$) | Tidal Range (m) | Tidal Phase | $L_e$ (km) |
|---|---|---|---|---|
| Nov. 20, 2008 | 608 | 1.19 | Flooding | 3.68 |
| | | | Flooding | 4.53 |
| | | | Flooding | 5.31 |
| | | | Flooding | 5.71 |
| | | | Flooding | 6.02 |
| | | | Flooding | 6.47 |
| | | | Flooding | 7.23 |
| | | | Flooding | 7.82 |
| | | | Flooding | 8.49 |
| | | | Flooding | 8.90 |
| | | | Ebbing | Not sampled |
| | | | Ebbing | Not sampled |
| | | | Ebbing | 7.99 |
| | | | Ebbing | 7.90 |
| | | | Ebbing | 7.90 |
| | | | Ebbing | 7.22 |

Table 3 continued.

| Date | Discharge ($m^3/s$) | Tidal Range (m) | Tidal Phase | $L_e$ (km) |
|---|---|---|---|---|
| June 16, 2011 | 702 | 1.21 | High-slack water | 7.55 |
| | | | Low-slack water | 3.22 |
| June 21, 2011 | 340 | 1.00 | Low-slack water | 5.17 |
| | | | Flooding | 7.24 |
| | | | High-slack water | 10.08 |
| June 27, 2011 | 852 | 0.96 | High-slack water | 6.35 |
| | | | Ebbing | 5.48 |
| | | | Low-slack water | 4.56 |
| July 6, 2011 | 334 | 1.20 | Low-slack water | 5.17 |
| | | | Flooding | 7.00 |
| | | | High-slack water | 10.75 |

Table 4: Summary of discharge and tidal conditions during June/July 2011.

| Date | Discharge ($m^3/s$) | Tidal Range (m) | Tidal Phase | $L_e$ (km) |
|---|---|---|---|---|
| Nov. 16, 2009 | 773 | 1.37 | Ebbing | Not sampled |
| | | | Ebbing | 5.16 |
| Nov. 17, 2009 | 799 | 1.31 | Ebbing | Not sampled |
| | | | Ebbing | Not sampled |
| | | | Ebbing | Not sampled |
| | | | Ebbing | Not sampled |
| | | | Ebbing | Not sampled |
| | | | Ebbing | Not sampled |
| | | | Ebbing | Not sampled |
| Nov. 19, 2009 | 654 | 1.16 | Ebbing | Not sampled |
| | | | Ebbing | Not sampled |
| | | | Ebbing | Not sampled |
| | | | Ebbing | Not sampled |
| | | | Ebbing | Not sampled |
| | | | Ebbing | Not sampled |
| | | | Ebbing | Not sampled |
| | | | Ebbing | Not sampled |
| | | | Ebbing | Not sampled |
| | | | Ebbing | Not sampled |
| | | | Ebbing | Not sampled |

Table 5: Summary of discharge and tidal conditions during November 2009.

The length of an estuary ($L_e$), or the farthest distance upstream that seawater intrudes, varies as a function of discharge (Dyer, 1997). The maximum distance of salt intrusion for a study day was determined to be the farthest upstream intersection of the 2 psu isohaline with the bed (Howard-Strobel et al., 1996). Transects from the four high-slack water transects from June/July 2011 and the high-slack water transects from November 17 and 18, 2008 were used to determine the relationship between $L_e$ and discharge (Figure 8).

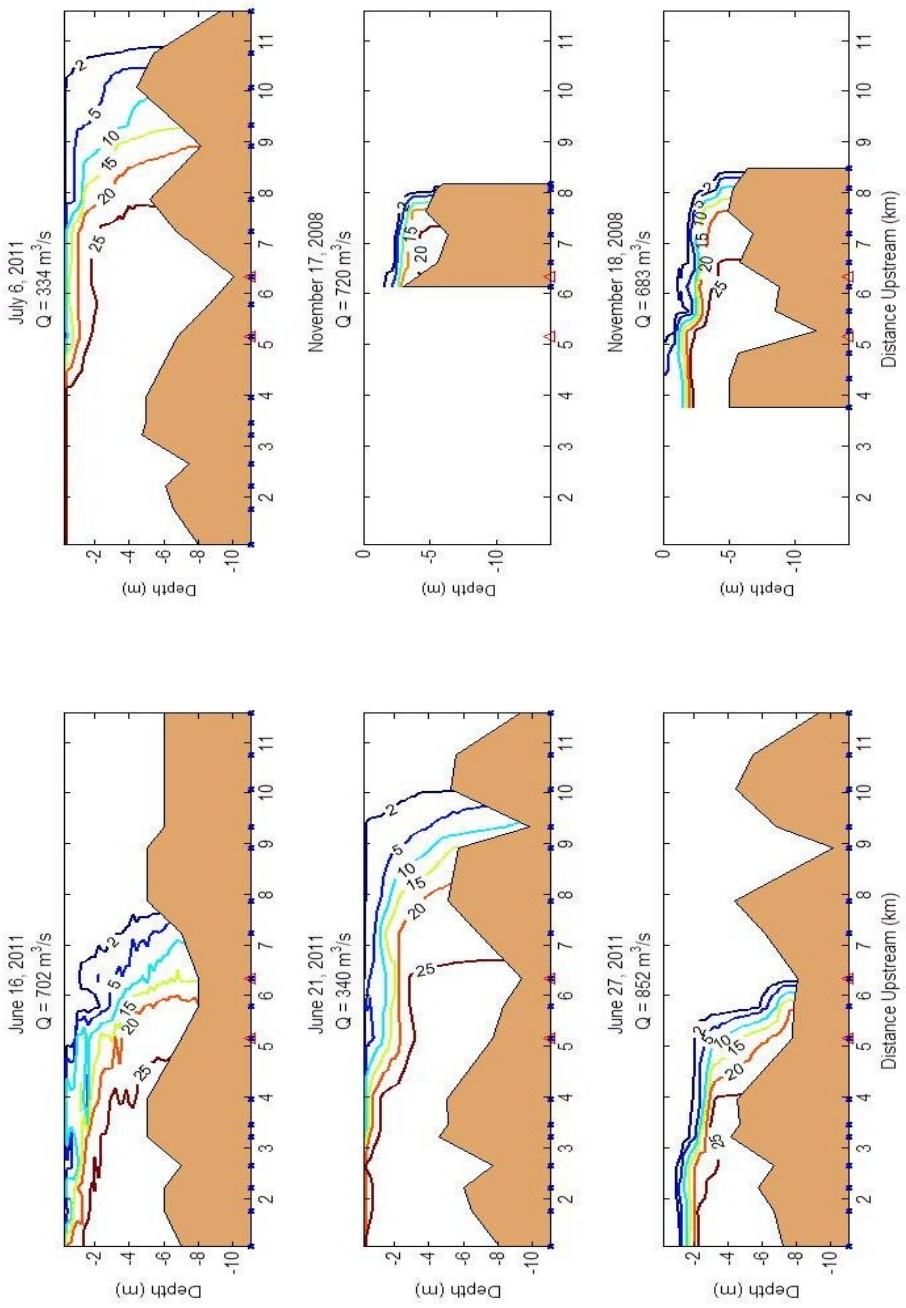


Figure 8: Salinity distribution in the Connecticut River estuary at high slack-water for various discharges. Transects are from June/July 2011 and November 2008.

A linear regression analysis (Figure 9) determined this relationship to be:

$$L_e = -0.0056 * Q + 12.6 \quad \textbf{(11)}$$

where $L_e$ is measured in kilometers and Q is river discharge ($m^3/s$). Using Equation 6, a hypothesis test was used to test the significance Equation 11. With a t-score of 1.81 and n = 6, this relationship is significant at a 90% level of statistical significance.

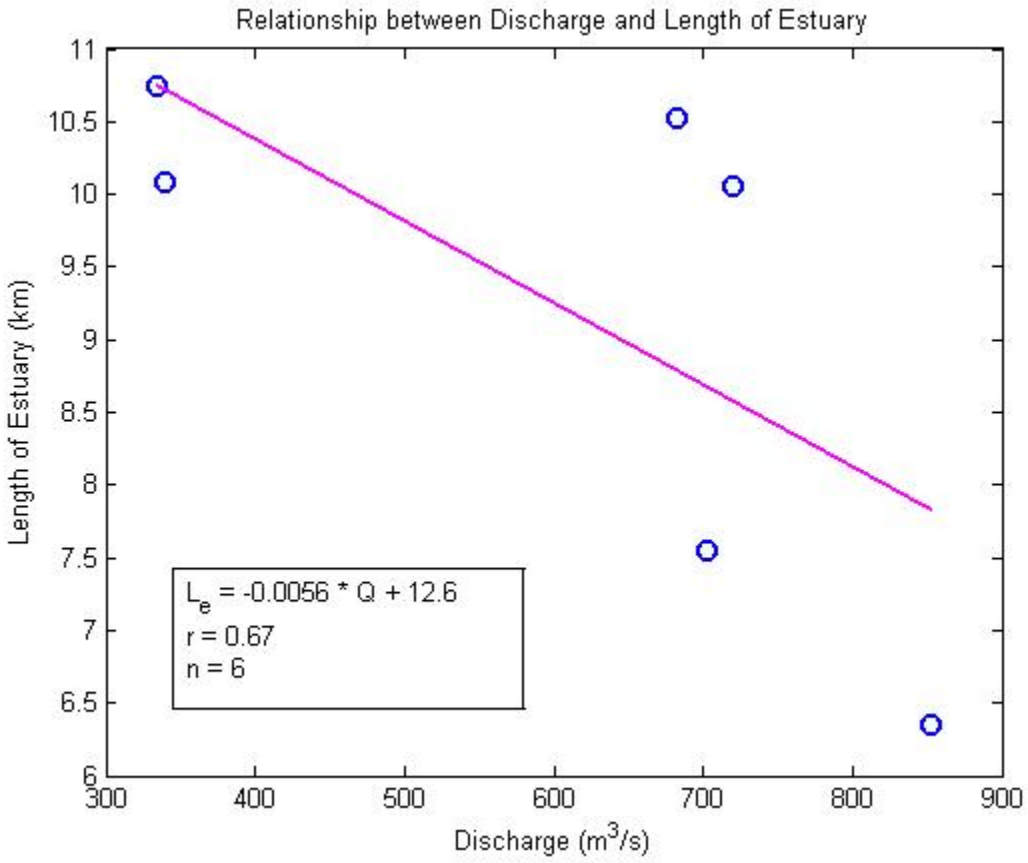


Figure 9: Linear regression analysis of the relationship between length of estuary (Le) in km and river discharge (Q) in m3/s.

This relationship suggests that Q sets the landward limit of salt intrusion and that under extremely high Q, the estuary may be completely flushed of salt water, which occurs during freshet in the Connecticut River estuary (Lemieux, 1983; Massad,1984).

### 5.2 Areas of Enhanced Suspended-Sediment Concentration

The position of the TM is associated with the maximum upstream position of the salt intrusion (Dyer, 1997). During the three study periods, there was often a measurable TM associated with the head of the salt intrusion (Figure 10 and Figure 11); however, areas of enhanced suspended-sediment concentration are also found downstream of the head of the salt intrusion (Figure 12, Figure 13 and Figure 14). The maximum suspended-sediment concentration was 454 mg/L and was observed during flood tide conditions on November 17, 2008 (Figure 14). In general, maximum concentrations on a given day were between 100-200 mg/L and occurred during flooding or ebbing currents, when tidal velocities are maximized and sediments are resuspended. Suspended-sediment concentrations were typically lower throughout the estuary at low-slack or high-slack water when sediments tend to settle out of suspension. During flooding or ebbing tides, surface to bottom concentrations typically vary by a factor of 15, from 10 mg/L to approximately 150 mg/L, at areas of peak concentrations; whereas, at slack water the surface to bottom concentration difference is usually a factor of 2 to 4, but can be up to 7 in the deeper areas of the estuary.

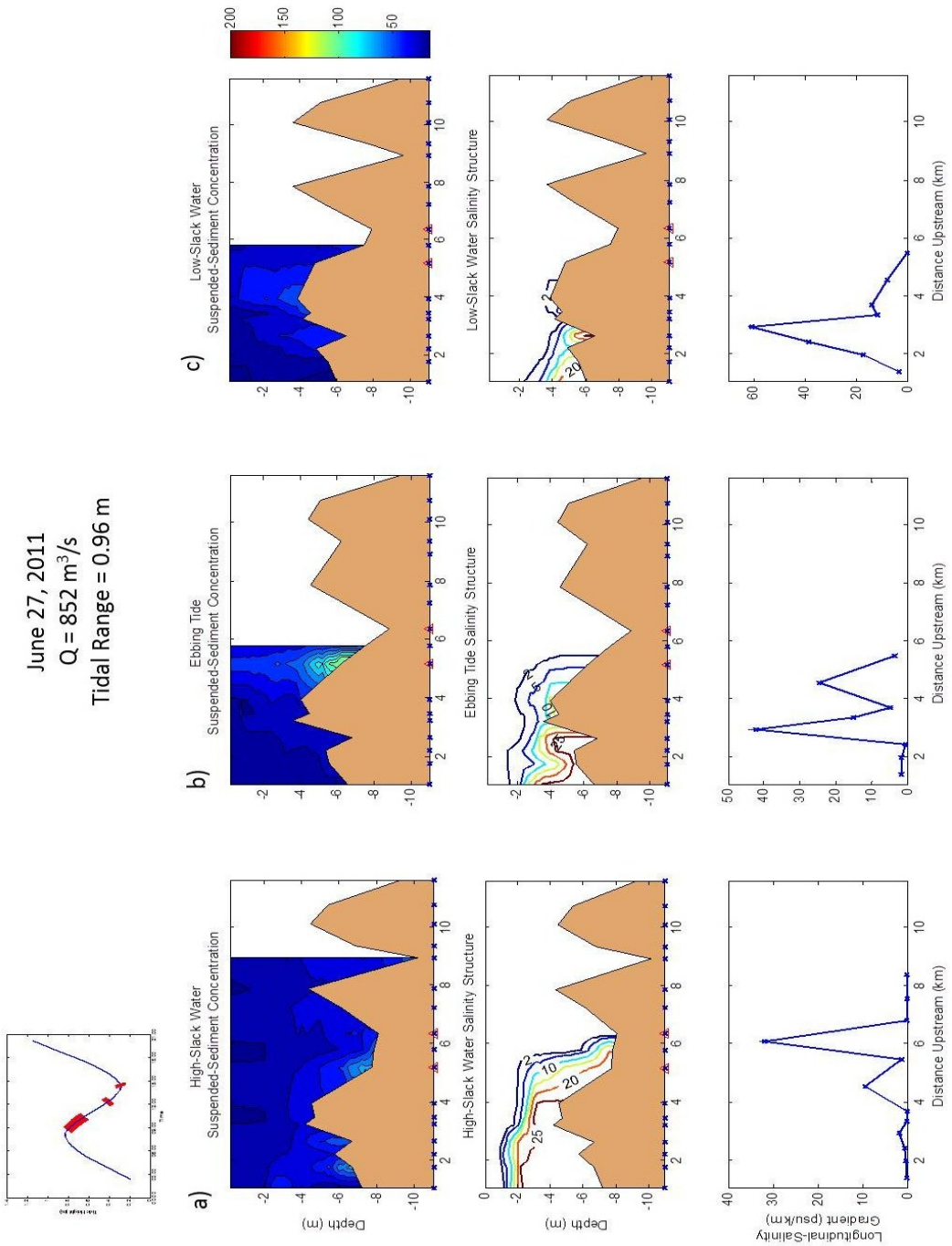


Figure 10: Suspended-sediment concentration, salinity and longitudinal salinity gradient transects from (a) high-slack water, (b) ebbing tide, and (c) low-slack water on June 27, 2011.

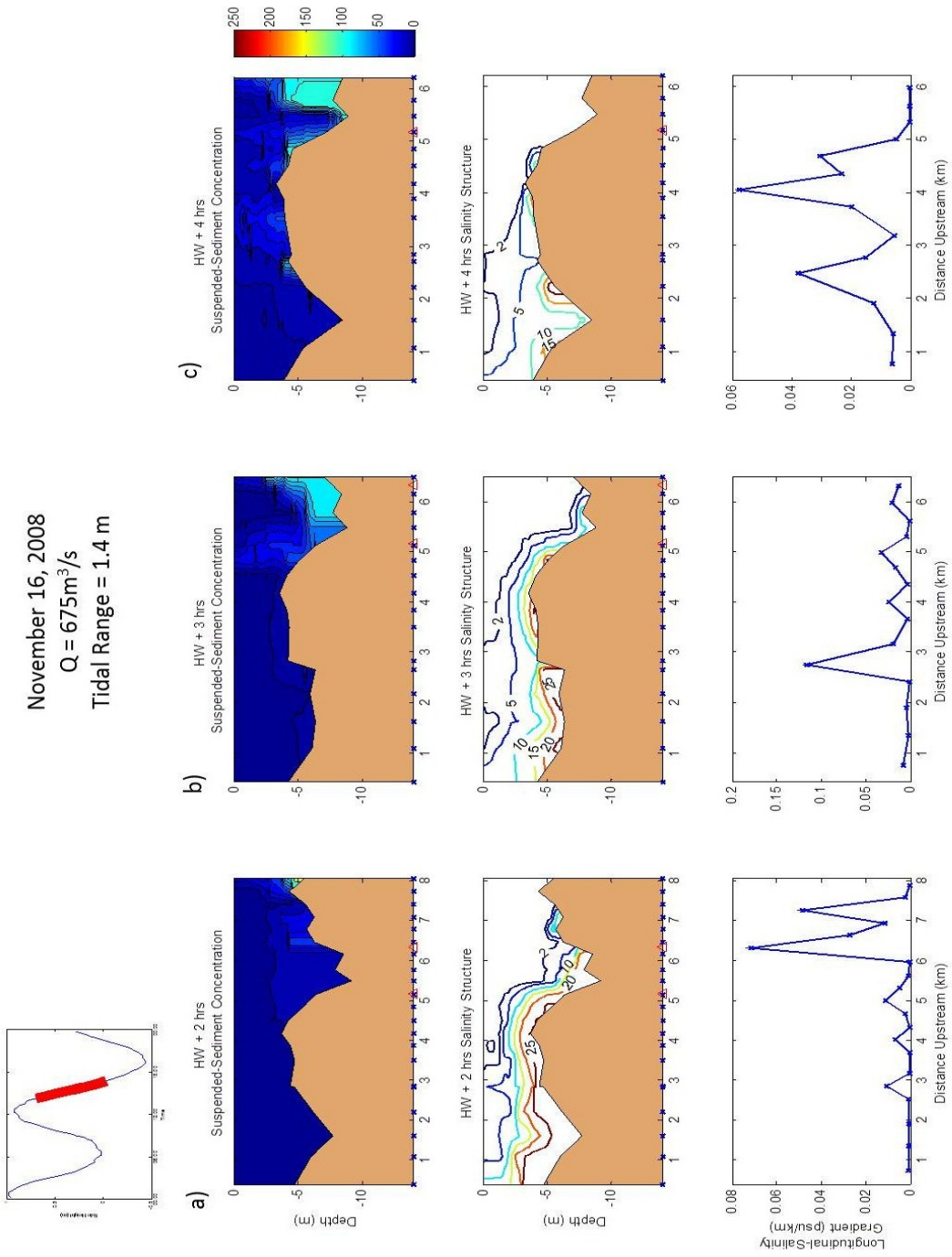


Figure 11: Suspended-sediment concentration, salinity and longitudinal salinity gradient transects from (a) high-slack water, (b) ebbing tide, and (c) low-slack water on November 16, 2008.

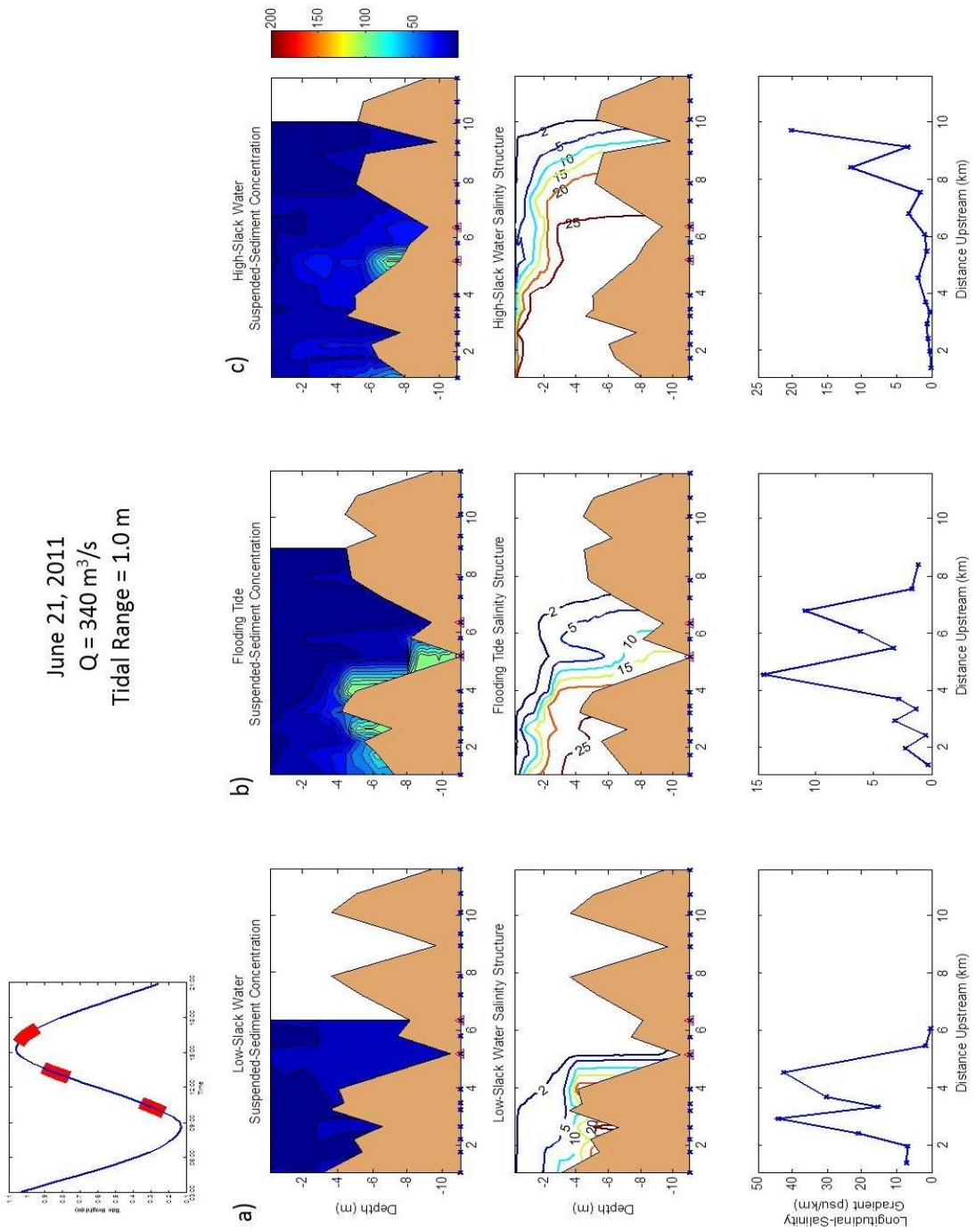


Figure 12: Suspended-sediment concentration, salinity and longitudinal salinity gradient transects from (a) high-slack water, (b) ebbing tide, and (c) low-slack water on June 21, 2011.

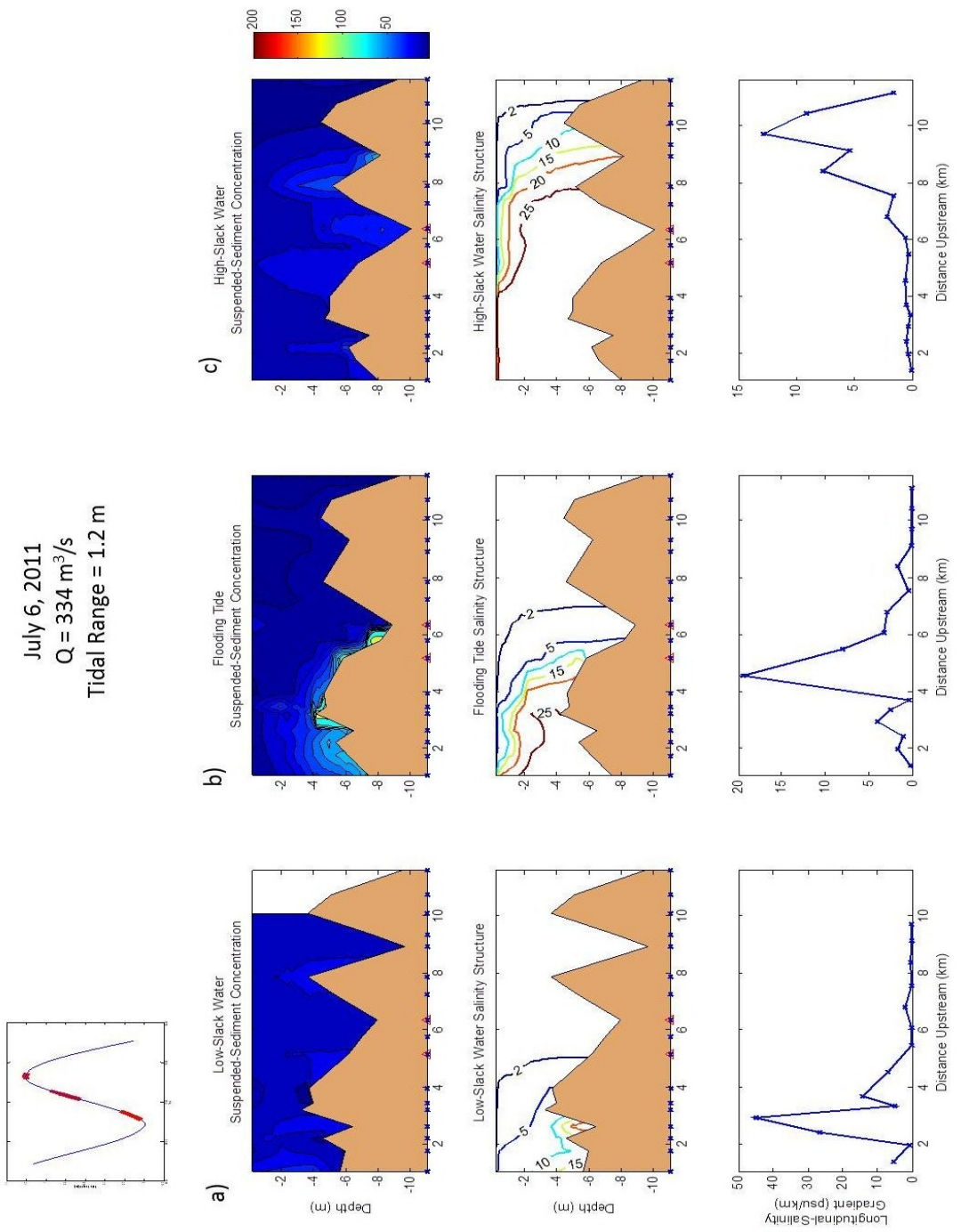


Figure 13: Suspended-sediment concentration, salinity and longitudinal salinity gradient transects from (a) high-slack water, (b) ebbing tide, and (c) low-slack water on July 6, 2011.

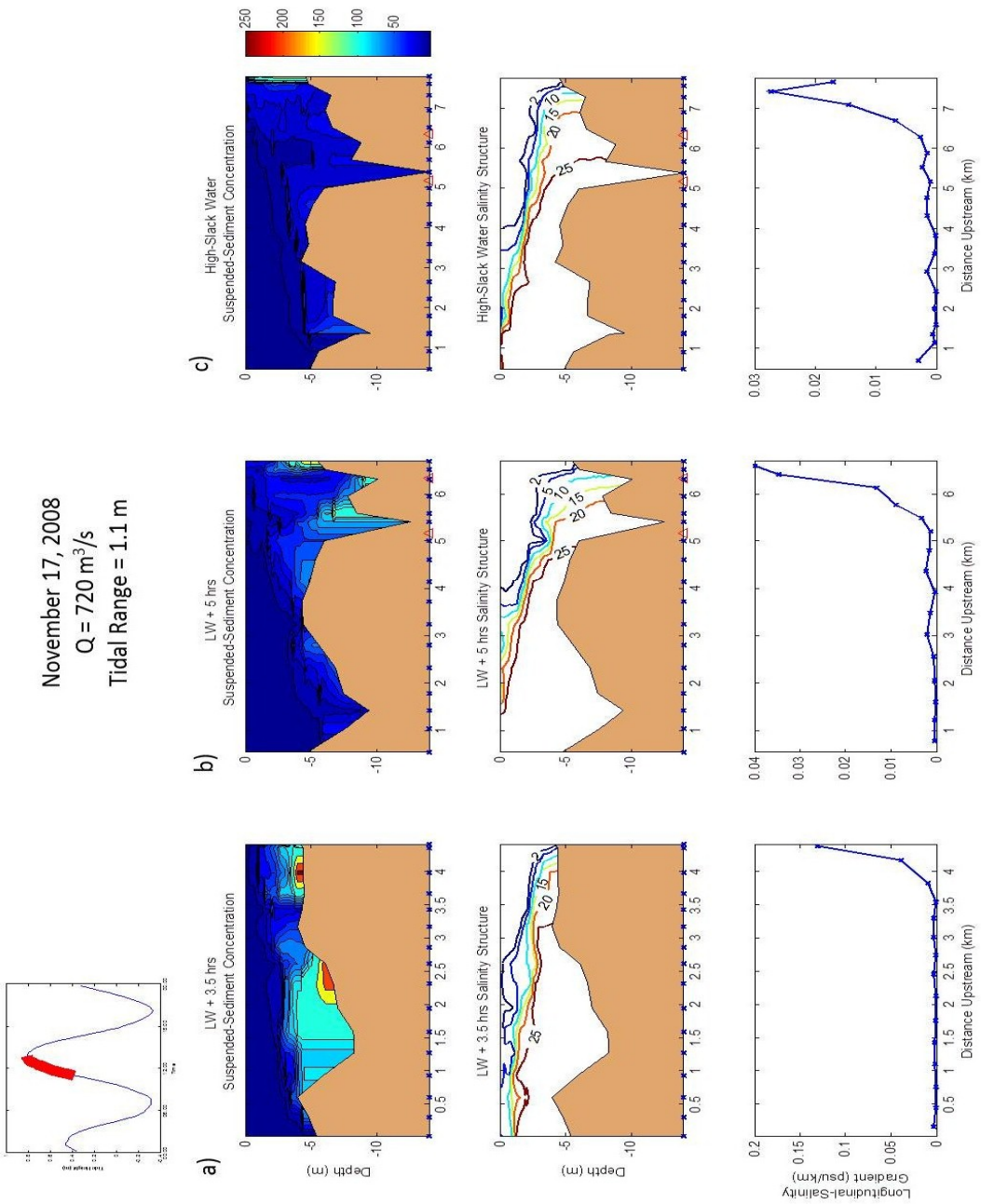


Figure 14: Suspended-sediment concentration, salinity and longitudinal salinity gradient transects from (a) high-slack water, (b) ebbing tide, and (c) low-slack water on November 19, 2008.

Transects with an observable intersection of the 2 psu isohaline and the bed were used to perform a linear regression analysis of the relationship between $L_e$ and the position of the TM (Equation 12; Figure 15):

$$X_{TM} = 0.94 * L_e - 1.15 \quad \textbf{(12)}$$

where $X_{TM}$ is position of the turbidity maximum (km). As described above, a t-test was performed to determine the significance of this relationship. With a t-score of 7.83 and n = 44, this relationship is significant at the 99% level of statistical significance.

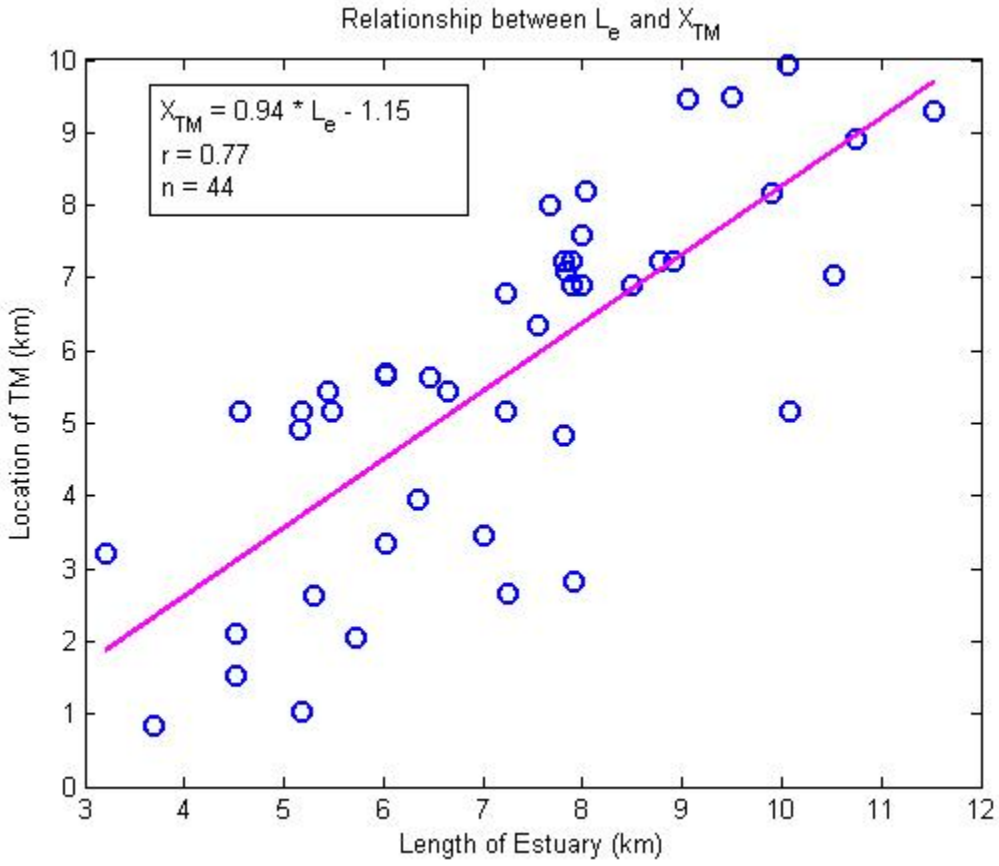


Figure 15: Linear regression analysis of the relationship between Le and position of the primary estuarine turbidity maximum.

Spearman's rank correlation coefficient, $r_s$, was also calculated (Equation 13) to further test the significance of this relationship.

$$r_s = \frac{S_{xy}}{\sqrt{S_{xx}S_{yy}}} \quad \textbf{(13)}$$

where $x_i$ and $y_i$ represent the ranks of the *i*th pair of observations and $S_{xy}$, $S_{xx}$, and $S_{yy}$ are defined as:

$$S_{xy} = \Sigma x_i y_i - \frac{(\Sigma x_i)(\Sigma y_i)}{n_o} \quad \textbf{(14)}$$

$$S_{xx} = \Sigma {x_i}^2 - \frac{(\Sigma x_i)^2}{n_o} \quad \textbf{(15)}$$

$$S_{yy} = \Sigma {y_i}^2 - \frac{(\Sigma y_i)^2}{n_o} \quad \textbf{(16)}$$

where $n_o$ is the number of ranked pairs. With $r_s$= 0.43, this test also proves this relationship to be significant at the 99% level of statistical significance. This relationship verifies that a TM exists at the classical location in the Connecticut River estuary.

In addition to the TM at the head of the salt intrusion, the Connecticut River estuary exhibited areas of enhanced suspended-sediment concentration downstream of the head of the salt intrusion. These areas were typically located in the deeper part of the estuary, found at approximately 5 km, in association with peaks in the longitudinal salinity gradient (Figure 12, Figure 13 and Figure 14). A linear regression was performed to determine the relationship between the location of these secondary TMs and the location of peaks in the longitudinal salinity gradients (Equation 17; Figure 16).

$$\mathrm{X_{STM}} = 0.72 * \mathrm{X_F} + 0.98 \quad \textbf{(17)}$$

where $X_{STM}$ is the position of the secondary TM (km) and $X_F$ is the position of a longitudinal salinity gradient peak (km).

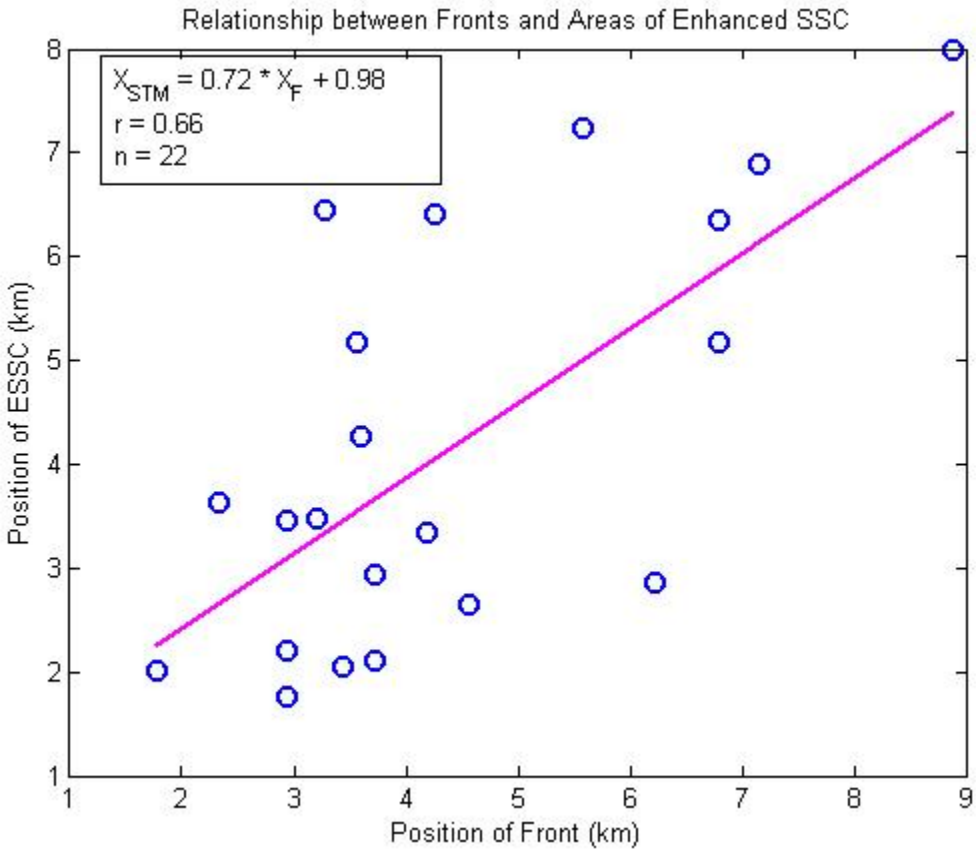


Figure 16: Linear regression analysis of the relationship between the position of secondary turbidity maximum and areas of secondary longitudinal-bottom salinity gradients.

As described above, a t-score and Spearman's rank correlation coefficient were calculated to determine the significance of this relationship. With a t-score of 3.90, $r_s = 0.53$, and n = 22, this relationship is significant at a 99% level of statistical significance. This suggests that in conjunction with a classical TM, the Connecticut River estuary experience areas of enhanced suspended-sediment concentration where there are peaks in the longitudinal salinity gradient.

### 5.3 Velocity and Suspended-Sediment Concentration

A peak in the longitudinal salinity gradient has been shown to be associated with the presence of an estuarine front (Simpson and Linden, 1989). In order to further examine the processes acting to focus sediments in these areas, suspended-sediment concentration and velocity transects from November 19, 2008 were examined (Figure 17 and Figure 18). During flood tide conditions, there is a 'jet' of high velocity, landward flowing water that coincides with the pycnocline, suggesting that the intermediate salinity waters of the pycnocline are flowing past the denser bottom waters as the salt wedge migrates upstream (Figure 17a and Figure 18a). This landward moving layer converges with slower moving water as it enters the deeper part of the estuary at 5.3 km, which is seen as a deceleration from 0.8 m/s at 5 km to 0.2 m/s at 5.3 km (Figure 18a). The corresponding suspended-sediment concentration transect shows that suspended-sediment concentrations increase within the slower waters, suggesting that sediment is resuspended in shallow areas and carried to the deeper parts of the estuary where it settles out of suspension as flow velocity decreases (Figure 17a).

When the tide turns, surface waters begin to ebb before and reach higher velocities than bottom waters (Figure 18b). In the deep section of the estuary, surface waters ebb at approximately 1.4 m/s while bottom waters are effectively stagnant, therefore enhancing vertical stratification. Suspended-sediment concentrations on the ebb tide, in this part of the estuary, are 5 to 10 times lower than those observed during flood tide (Figure 17b). This is likely due to enhanced stratification and low velocity bottom water, which both suppress turbulent mixing and limit sediment resuspension, respectively (Geyer, 1993).

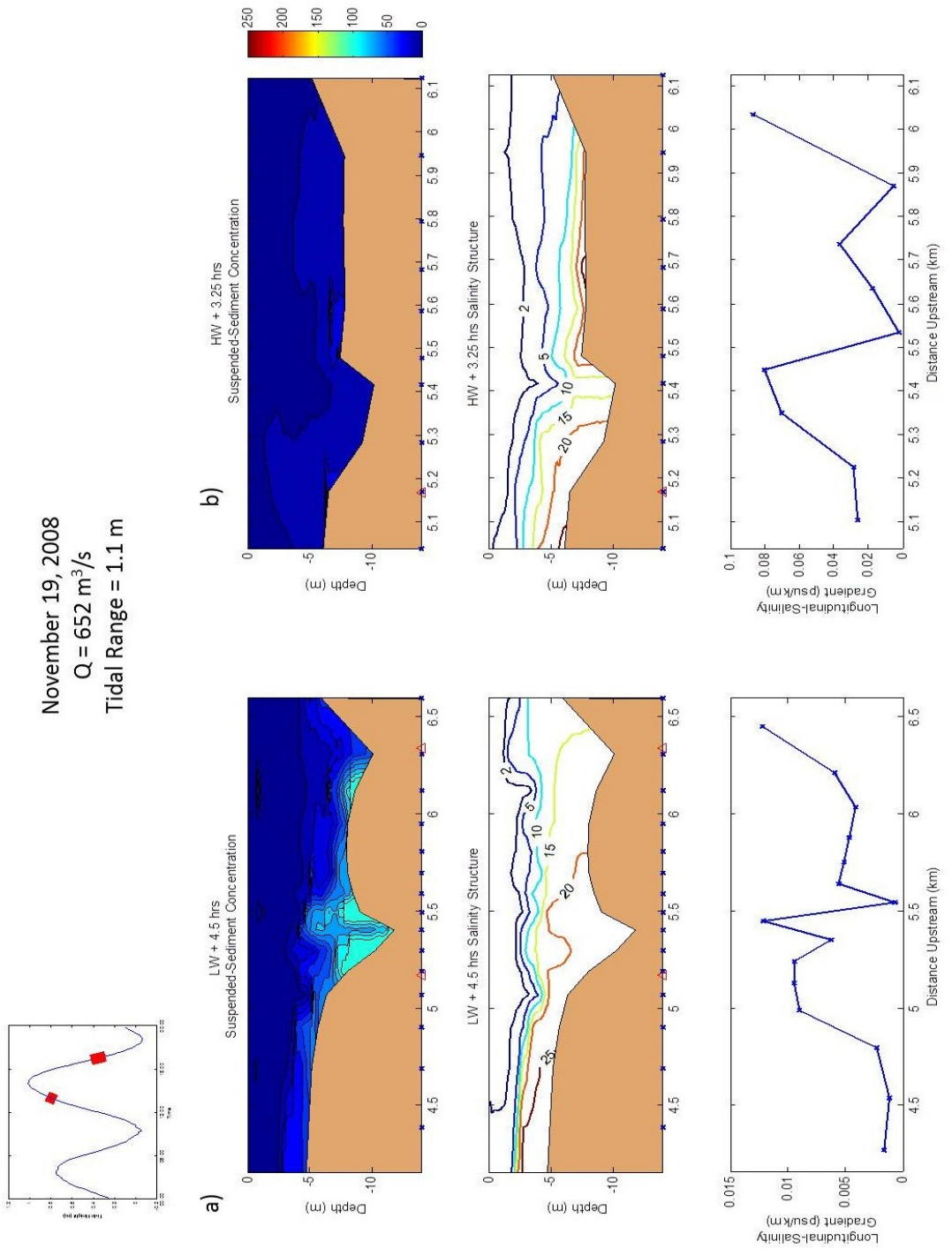


Figure 17: Suspended-sediment concentration, salinity and longitudinal salinity gradient transects from (a) low water + 4.5 hours (flooding tide) and (b) high water + 3.25 hours (ebbing tide) on November 19, 2008.

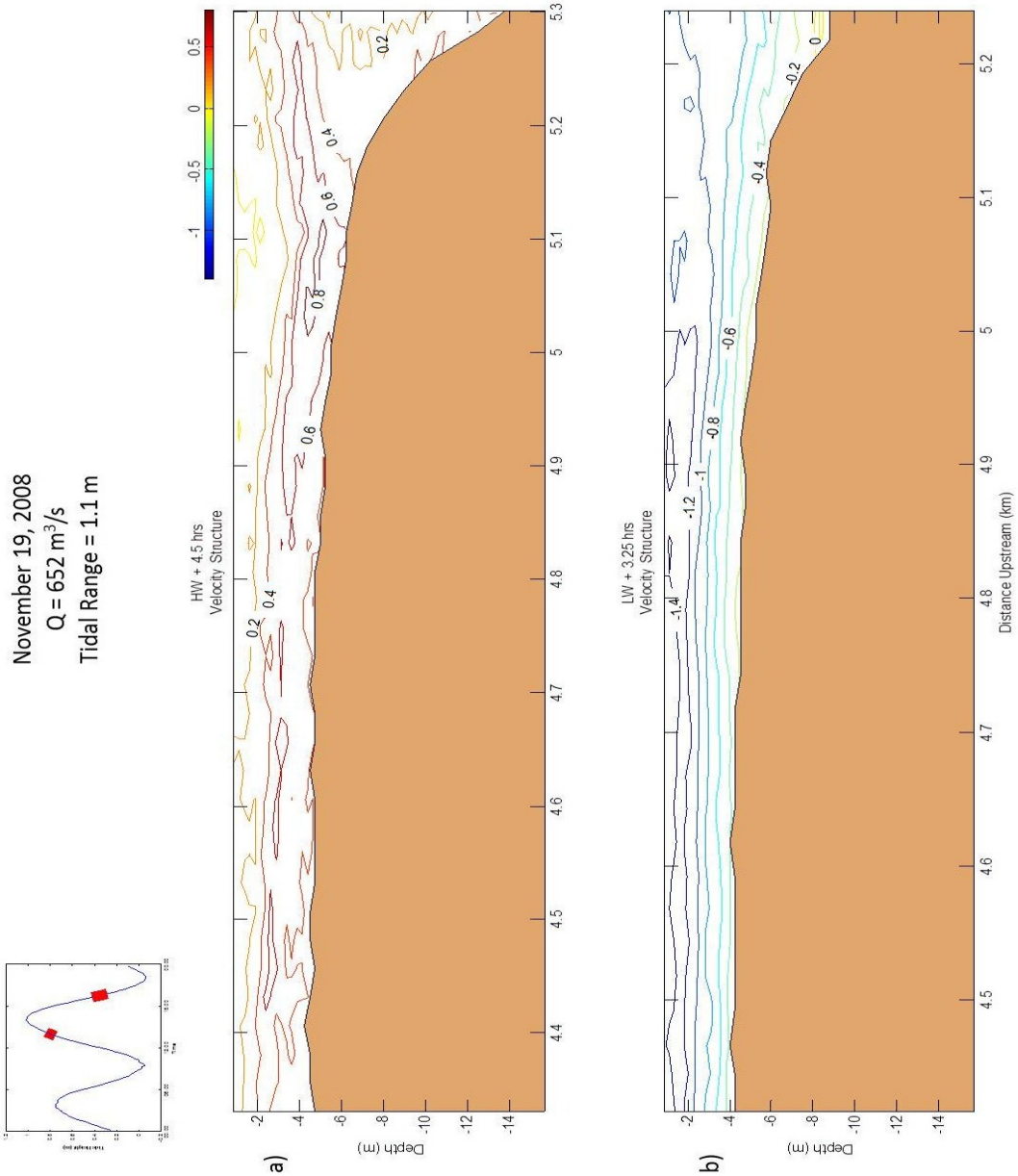


Figure 18: Velocity transects from (a) low water + 4.5 hours (flooding tide) and (b) high water + 3.25 hours (ebbing tide) on November 19, 2008.

## 6. Discussion

### 6.1 Variability of Suspended-Sediment Distribution

Suspended-sediment concentration is highly variable throughout the Connecticut River estuary; however, certain areas persistently have increased suspended-sediment concentration during all phases of the tide. Previous studies have shown that a TM exists in the Connecticut River estuary and that suspended-sediment concentration within this feature is approximately 60-70 mg/L, although concentrations may be as low as 20 mg/L (Massad, 1984; Bohlen, 1996). This range of concentrations was used to define areas of enhanced suspended-sediment concentration as either a primary TM, where the maximum concentration was, or as a secondary TM, areas other than the primary TM with concentrations greater than 20 mg/L. Although the majority of concentrations found in this study are higher than previous studies they are considered to be within reason because Lemieux (1983) showed that under similar discharge conditions suspended-sediment concentration in the Connecticut River estuary can reach approximately 600 mg/L.

The concentration within both primary and secondary TMs fluctuates with the semidiurnal tides. Suspended-sediment concentrations peak during flooding and ebbing tides when tidal current velocities are maximized and therefore bed shear stress and sediment resuspension are greatest; concentrations diminish at high and low-slack water as tidal velocities are minimized and particles settle out of suspension. Because both a classical TM that migrates with the salt intrusion and secondary TMs downstream of this feature exist, it is likely that a combination of advection and resuspension processes are occurring in the Connecticut River estuary. Furthermore, secondary TMs are consistently found in deeper parts of the estuary,

particularly at 5.3 km, implying that there are other factors acting to focus sediment at this location, such as flow convergence or changes in bottom sediment type.

To examine the role of flow convergence, the longitudinal salinity gradient (ds/dx) was calculated for each salinity transect. Primary and secondary TMs form in association with peaks in the salinity gradient (Figure 10a-c, Figure 12a-c, and Figure 13a-c). A sharpening of the longitudinal salinity gradient is representative of an estuarine front (Simpson and Linden, 1989). While the head of the salt intrusion is known to be a zone of flow convergence (Dyer, 1997), fronts also form downstream of channel constrictions and sills where the channel widens or deepens (Kineke, 2001; Largier, 1992). Velocity transects at 5.3 km show that flow convergence is occurring on the flood tide in the deeper parts of the estuary (Figure 18a). During ebb tide conditions, near zero velocities exist in the bottom waters and vertical stratification is intensified which reduces turbulent mixing and increases vertical particle settling rates (Geyer, 1993). The combination of these processes acts as sediment trap through convergence of near-bottom and surface flow and enhanced particle settling.

Geyer's theoretical equations for density-dependent frontogenesis were used to determine if frontogenesis conditions were observed in the Connecticut River estuary. Calculations were performed during waning ebb conditions, when frontogenesis is suggested to occur, and during flood conditions (Kineke et al., 2000). Due to the limits of this data set, several assumptions and estimations were used in these calculations. In Equations 1 and 3, $U_T$ was assumed to equal 0.6 m/s (Garvine, 1975; Ralston et al., 2010). To calculate the longitudinally-varying $U_T$ in Equation 2 a cross-sectional area was calculated using the depth at 5.1 km (~6.5 m) and a width equal to 460 m (Lemieux, 1983). This area was then used to calculate the discharge through this cross section:

$$Q_T = U_T * A \quad (\mathbf{18})$$

where $Q_T$ is the tidal discharge (m/s) and A is the cross-sectional area ($m^2$). The cross-sectional area at 5.3 km was then calculated using the depth at that station (~9.4 m) and 460 m for the width. Assuming conservation of mass and momentum, Equation 15 was used to calculate $U_T$ at 5.3 km by dividing the calculated $Q_T$ by A at 5.3 km (Dyer, 1997). After calculating $U_T$ at 5.1 and 5.3 km, a longitudinally-varying $U_T$ was calculated and used to solve Equation 2.

For ebb conditions, equations 1, 2, and 3 yielded a stratification term of 0.5, an adverse pressure gradient scaling of 6, and a baroclinic pressure gradient scaling of 3, respectively. Calculations for flood conditions yielded a stratification term of 0.5, an adverse pressure gradient scaling of 7, and a baroclinic pressure gradient scaling of 20. These values satisfy two of the three theorized conditions for frontogenesis (Equations 2 and 3). The stratification term (Equation 1) was not satisfied, which may be due to the average tidal velocity that was used in calculations; however, it could also mean that frontogenesis can occur under more stratified conditions than originally hypothesized. With two of the three conditions satisfied, it is likely that frontogenesis is occurring in the Connecticut River estuary and is responsible for trapping sediments in deeper parts of the estuary.

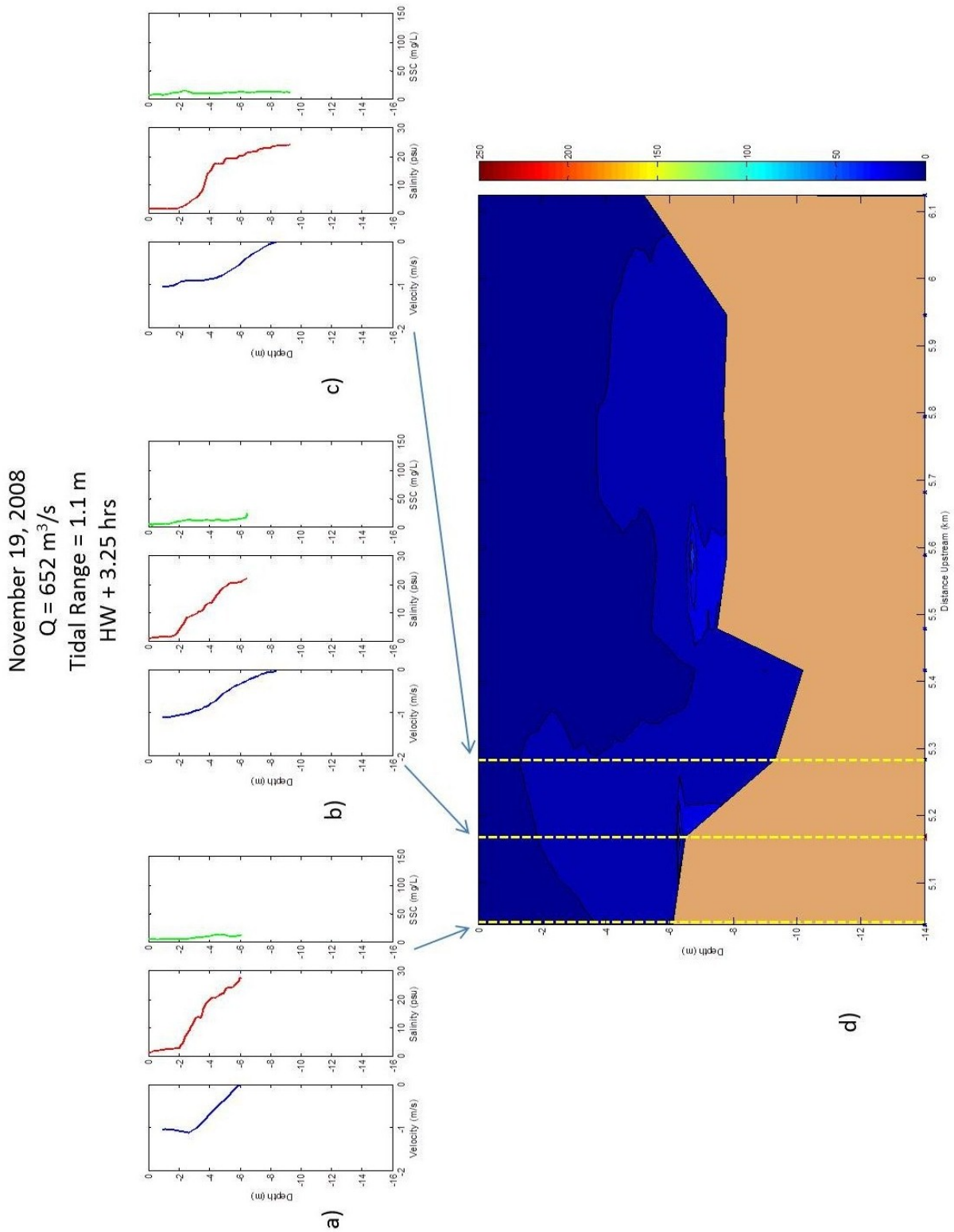


Figure 19: Vertical profiles of velocity (blue), salinity (red) and suspended-sediment concentration (green) at (a) 5.1 km, (b) 5.2 km and (c) 5.3 km upstream of the estuary mouth and (d) corresponding suspended-sediment concentration transect during ebb conditions on November 19, 2008.

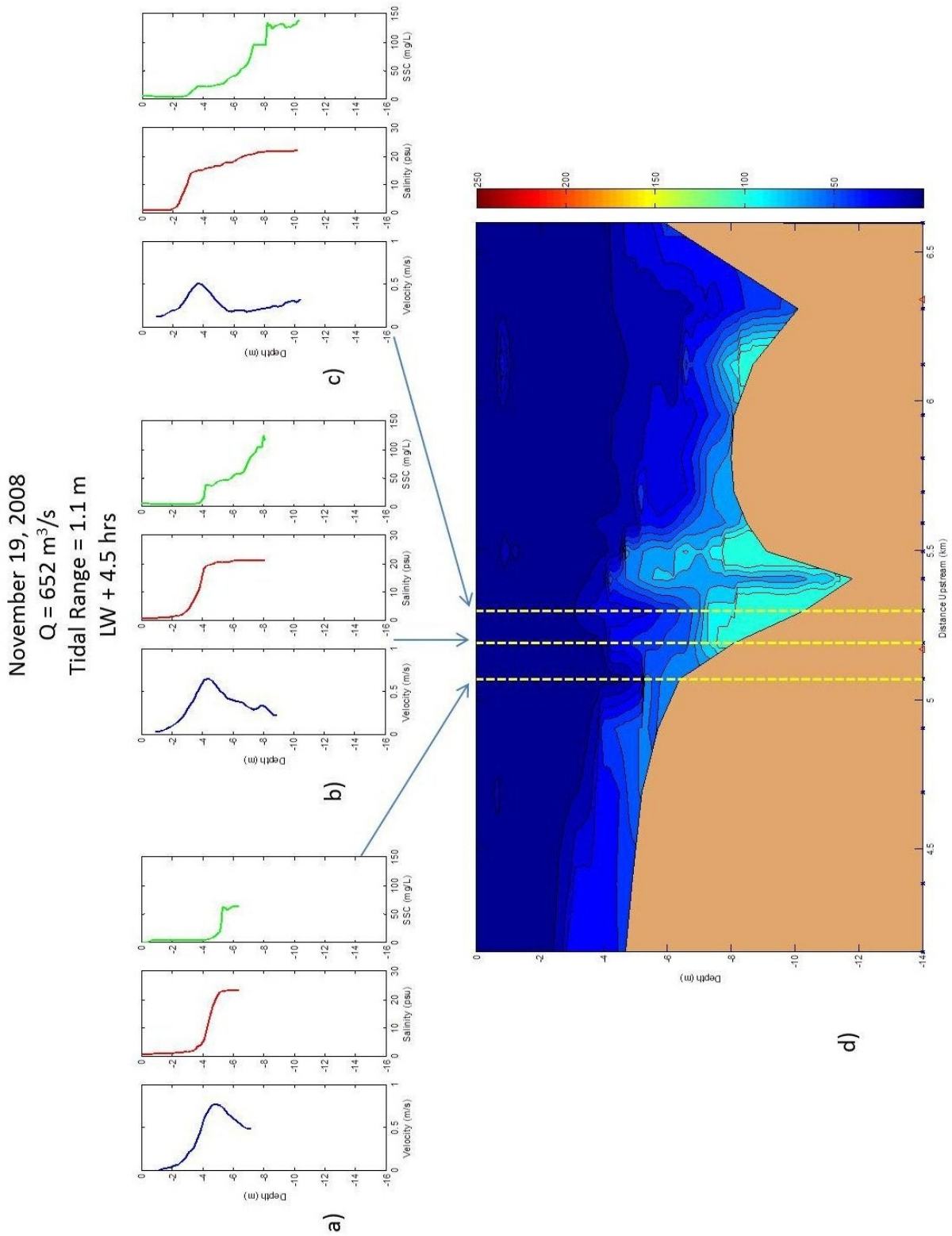


Figure 20: Vertical profiles of velocity (blue), salinity (red) and suspended-sediment concentration (green) at (a) 5.1 km, (b) 5.2 km and (c) 5.3km upstream of the estuary mouth and (d) corresponding suspended-sediment concentration transect during flood conditions on November 19, 2008.

### 6.2 Suspended Sediment Fluxes

Lemieux (1983) suggested that the Connecticut River estuary is an effective sediment trap and Horne and Patton (1989) identified a nodal point at approximately 5-6 km where bed material could be stored temporarily. Using velocity and suspended-sediment concentration data from November 19, 2008 (Figures 19a-d and Figure 20a-d) an instantaneous flux was calculated for flood and ebb tide conditions at 5.1 km and 5.3 km:

$$F = \int_0^h uc\, dz \qquad (\mathbf{19})$$

where F is flux (mg/s/m), h is total water depth (m), c is suspended-sediment concentration (mg/L) and dz is bin size (m). Fluxes for max flooding currents (FF) and max ebbing currents (EF) are summarized in Table 6.

| | Flood Flux (mg/s/m) | Ebb Flux (mg/s/m) | Total Depth (m) |
|---|---|---|---|
| 5.1 km | 46.3 | -25.0 | 6.3 |
| 5.3 km | 146.1 | -52.7 | 10.4 |
| Difference | 99.8 | 27.7 | 4.1 |

Table 6: Summary of suspended sediment flux calculation. Negative sign denotes seaward transport.

Comparison of FFs shows an approximate 100 mg/s/m increase in suspended-sediment flux in the deep part of the estuary. This increase in flux could be explained by the greater depth at 5.3 km (Table 6) or by physical processes acting at this location. According to the law of conservation of mass, the total flux through a given cross-sectional area upstream should be the same as the flux through another cross-sectional area downstream (Dyer, 1997). Assuming that the width at the two stations is the same, cross-sectional area is dependent on depth. Therefore, the water column at 5.3 km can be divided into two sections, an upper section with the same depth and cross-sectional area as the 5.1 km station, and a lower section with a cross-sectional

area equal to the remaining area of the channel. Theoretically, the FF through the upper section at 5.3 km should equal the FF through 5.1km; however, the upper section FF is 25.4 mg/s/m, which is less than the FF at 5.1 km (Table 6). This difference suggests that a process is acting to focus sediment in the lower water column. Maximum velocity at 5.1 km is 0.79 m/s and occurs 4.25 m; the velocity at 5.3 km at the same depth is 0.30 m/s (Figure 19a and Figure 19c). This deceleration of velocity in the deeper part of the estuary is representative of flow convergence associated with an estuarine front and is likely responsible for creating a downward flux that removes sediment from the upper water column.

Separation of the EF at 5.3 km into an upper and lower section shows that there is a seaward directed flux in the upper 6 m and a small landward flux, approximately 0.4 mg/s/m, in the lower 2.8 m (Figure 20d). This vertical profile of EF corresponds to enhanced stratification and minimal suspended-sediment concentrations observed in the deep part of the estuary during ebb conditions. Furthermore, a landward directed EF, although nearly zero, suggests that there is net sediment trapping in this section of the estuary.

### 6.3 Comparisons

Geyer's (2010) classification scheme was used to further classify the Connecticut River estuary for each study period. Representative values of $U_t$, tidal velocity, and $b_o$, baroclinic velocity, were taken from Ralston et al. (2010). $U_t$ was equal to 0.6 m/s and $b_o$ was equal to 1.5 m/s. It should be noted that:

$$b_o = \sqrt{g * \beta * s_{oc} * H} \quad \textbf{(20)}$$

where g, gravitational acceleration, is 9.8 $m/s^2$, β, the coefficient of expansivity for salinity is $7.7*10^{-4}$ $psu^{-1}$, $s_{oc}$, oceanic salinity, is 28 psu, and H, estuary depth, is 7 m. Varying Q over the

observed discharges (334 to 852 $m^3/s$) yielded a range of values for $U_r/b_o$ ($\frac{river\ velocity\ (\frac{m}{s})}{baroclinic\ velocity\ (\frac{m}{s})}$) from 0.14 to 0.36. $U_t/b_o$, which is the other variable used in this classification, was equal to 0.4. These values classify the Connecticut River estuary as highly stratified for all study periods. Other estuaries that plot in the vicinity of the Connecticut River estuary are the Hudson River estuary during high discharge, the Fraser River estuary and the Merrimack River estuary, suggesting that these estuaries should be comparable (Geyer, 2010).

The presence of a velocity 'jet' associated with the pycnocline has been shown to occur on the flooding tide in the Fraser estuary (Figure 21; Geyer and Farmer, 1989). Similar to the Merrimack, the Connecticut River estuary has been shown to range from a partially-mixed estuary to a more stratified, salt-wedge estuary with varying discharge (Horne and Patton, 1989). Data from the Merrimack also show that on the ebb, enhanced stratification at the head of the salt intrusion can create an adverse baroclinic pressure gradient that opposes the ebb and maintains near zero velocities in bottom waters downstream of the salinity front (Ralston et al., 2010). Similar velocity profiles from the Connecticut River estuary suggest that this may also be occurring on the ebb tide and could contribute to temporary sediment trapping in deep sections of the estuary.

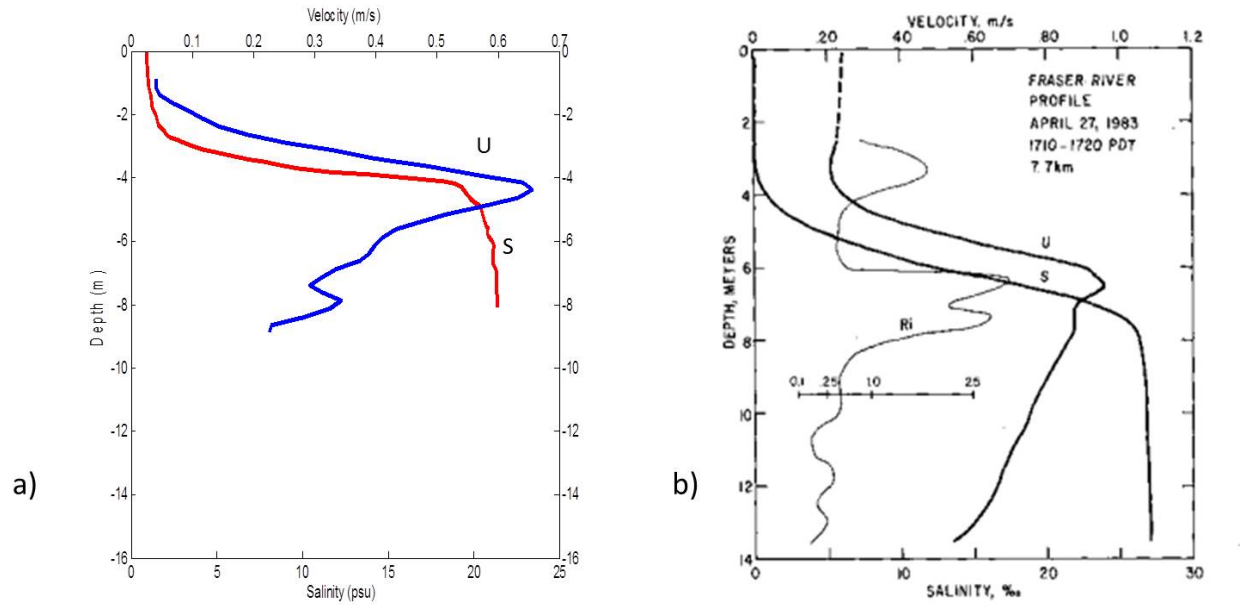


Figure 21: Vertical profiles of velocity (U) and salinity (S) from a) the Connecticut River estuary and b) the Fraser estuary (Geyer and Farmer, 1989). These profiles indicate the presence of a velocity jet associated with the pycnocline.

### 6.3 Future Research

Future research on the variability of suspended-sediment distribution in the Connecticut River estuary should incorporate time-series measurements from anchored instrument arrays in the lower, middle and upper sections of the estuary to observe the formation of fronts and associated TMs. These observations would also help to clarify conditions under which Geyer's theoretical conditions for frontogenesis are achieved. A longer study period, at different times of the year, would also help to increase understanding of how locations of fronts and TMs vary over a wider range of discharge and tidal conditions. Furthermore, higher-resolution and more in-depth measurements would allow for better comparison of the Connecticut River estuary with other estuaries worldwide.

## 7. Conclusions

Analysis of longitudinal transects conducted in the Connecticut River estuary during June/July 2011, November 2009 and November 2008 show that suspended-sediment concentration is highly variable, but there are certain areas that show persistent increased suspended-sediment concentrations relative to areas up and downstream. The areas of enhanced suspended-sediment concentration are associated with intensification of the longitudinal salinity gradient. During most phases of the tide there is a primary TM located at the head of the salt intrusion and secondary TMs located downstream in deeper parts of the estuary, typically 2-3 and 4-6 km. Sediment concentrations in the TMs vary over a semidiurnal tidal cycle, with maximum concentrations occurring during flooding tides when tidal velocities are maximized. Sediment is resuspended during the flooding tides and carried upstream to deeper parts of the estuary where flow convergence allows particles to settle out of suspension. Decreased velocities and enhanced stratification following the flood effectively focus fine sediments in these locations.

Understanding where TMs form and the processes that create these features is important because of their potential to trap sediments in specific locations. Continued formation of TMs at the same locations in an estuary will cause intensified deposition in these areas which can negatively affect navigation and lead to the need for dredging. Also, the surficial charges of fine sediments tend to attract heavy metals, such as mercury, dissolved in the water column. Over time, contamination will be concentrated with continued deposition in the same area and can cause harm to fish population and other biota in the estuary. Understanding the dynamics that create areas of enhanced suspended-sediment concentration can help to predict where these areas

of deposition and/or contamination will occur in an estuary and can give insight into how best to fix the problems they may cause.

**References**


Bohlen W. F., Morton E. T., Howard-Strobel M.M., Cohen D.R. (1996) A Field Investigation of the Turbidity Maximum in the Connecticut River Estuary. *Long Island Sound Research Conference 1996*.

Brown, E. and Park, D. (1999) Waves, Tides, and Shallow-Water Processes. Butterworth-Heinemann in association with The Open University, England.

Cameron, W. M. and Pritchard, D. W. (1963) Estuaries. In: *The Sea* (Ed. MN Hill), vol. 2, Wiley, New York, 306-324.

D&A Instrument Company (1991) Instruction Manual: OBS-1 & 3 Suspended Solids & Turbidity Monitor.

Dyer, K. (1997) Estuaries: A Physical Introduction. John Wiley & Sons, Chichester, England.

Garvine, R.W. (1975) The Distribution of Salinity and Temperature in the Connecticut River Estuary. *Journal of Geophysical Research*, vol. 80, 1176-1183.

Geyer, W. R. and Farmer D. M. (1989) Tide-Induced Variation of the Dynamics of a Salt Wedge Estuary. *Jounral of Physical Oceanography*, vol. 19, 1060-1072.

Geyer, W. R. (1993) The Importance of Suppression of Turbulence by Stratification on the Estuarine Turbidity Maximum. *Estuaries*, vol. 16, no. 1, 113-125.

Geyer, W. R. (2010) Estuarine salinity structure and circulation *in* Contemporary Issues in Estuarine Physics. Cambridge University Press, Cambridge. 12-26.

Gordon, R. B. (1980) The sedimentary system of Long Island Sound *in* Estuarine physics and chemistry: Studies in Long Island Sound: Advances in Geophysics, ed. Saltzman, B., vol. 22, 1-35.

Hansen, D. V. and Rattray, M. Jr. (1966) New dimensions in estuary classification. *Limnology and Oceanography*, vol. 11, 319-326.

Horne, G. S. and Patton, P. C. (1989) Bedload-sediment transport through the Connecticut River estuary. Geological Society of America Bulletin, vol. 101, 805-819.

Howard-Strobel, M. M., O'Donnell, J., Bohlen, W. F., Cohen, D. R. (1996) Observations on the Hydrography of the Connecticut River During High and Low River Discharges. *Long Island Sound Research Conference 1996,* 32-41.

Kineke, G. C., Geyer, W. R., Milligan, T. G., Alexander, C. R., Ramsey, A. L., Blake, A. C. (2001). Sediment trapping and localized mud accumulation in two estuaries, southeastern US; Geological Society of America, 2001 annual meeting. *Abstracts with Programs - Geological Society of America, 33*(6), 405.

Kineke, G. C., Geyer, W. R., and Ramsey A. L. (2000). Sediment Trapping at Estuarine Fronts. 10th International Biennial Conference on Physics of Estuaries and Coastal Seas, Extended Abstracts. October 7-11, 2000, Norfolk, Virginia. SRAMSOE Report No. 366, Virginia Institute of Marine Science, Gloucester Point, VA, USA, pp. 316-319.

Largier, J. L. (1992) Tidal intrusion fronts. *Estuaries*, vol. 15, no. 1, 25-39

Lemieux, C. R. (1983) Suspended Sediment Transport in the Connecticut River Estuary. B.A. Thesis, Wesleyan University.

Lin, J. and Kuo, A. (2001). Secondary turbidity maximum in a partially mixed microtidal estuary. *Estuaries*, vol. 24, p. 707-720.

Massad, E. H. (1984) Suspended Sediment Patterns in the Connecticut River Estuary. B.A. Thesis, Wesleyan University.

Mendenhall W., Beaver R. J., Beaver B. M. (2009). Introduction to Probability and Statistics. Brooks/Cole, Cengage Learning. Belmont, CA, USA.

Partheniades, E. (2009). Cohesive Sediments in Open Channels, Elsevier, Inc., Oxford.

Pinet, R. P. (2000) Invitation to Oceanography: Second Edition. Jones and Barlett Publishers, Sudbury, MA, USA.

Ralston, D. K., Geyer, W. R., Lerczak, J. A., Scully, M. (2010) Turbulent mixing in a strongly forced salt wedge estuary. *Journal of Geophysical Research*.

Ralston, D. K., Geyer, W. R., Lerczak, J. A. (2010) Structure, variability and salt flux in a strongly forced slat wedge estuary. *Journal of Geophysical Research*. Vol. 115, C06005.

Simpson, J. E. and Linden, P. F. (1989) Frontogenesis in a fluid with horizontal density gradients. *Journal of Fluid Mechanics*, vol. 202, 1-16.

Schubel, J. R. and Kennedy, V. S. (1984) The Estuary as a Filter: An Introduction *in* The Estuary as a Filter, ed. Kennedy, V. S., Academic Press, Inc., Orlando, Florida, USA. 1-11.

Trujillo, A. P. and Thurman, H. V. (2011) Essentials of Oceanography: Tenth Edition. Pearson Education, Inc., Glenview, IL, USA.

Uncles, R. J., and Stephens, J. A., 1989. Distributions of suspended sediment at high water in a macrotidal estuary. *Journal of Geophysical Research*, vol. 94, 14395:14405.

Valle-Levinson, A. (2010) Definition and classification of estuaries *in* Contemporary issues in Estuarine Physics. Cambridge University Press, Cambridge. 1-11.

Woodruff, J. D., Naughton, T. J., Kekacs D. J., Elzidani, E., Martini, A. M. (in revision) Spatial and temporal trends in sediment trapping within floodplain waterbodies on a freshwater tidal river: Lower Connecticut River, USA. *Submitted to* Geological Society of America Bulletin.

## Appendix A

## June/July 2011

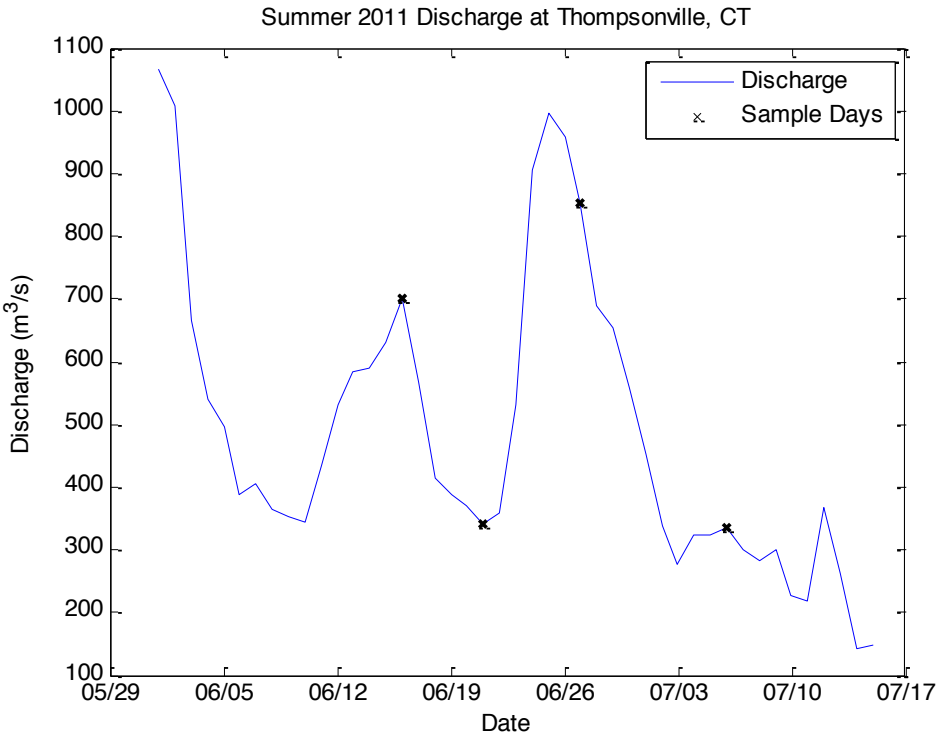


Figure A1: Discharge during the June/July 2011 study period. Discharge was measured at the USGS gage station on the Connecticut River at Thompsonville, CT.

| Date | Phase of Tide | Max SSC (mg/L) | Position of TM (km) | Position of Max Front (km) | STM (mg/L) | Position of STM (km) | Position of Secondary Front (km) |
|---|---|---|---|---|---|---|---|
| 6/16/ 2011 | High-Slack Water | 62.94 | 6.35 | 6.79 | Nan | Nan | Nan |
| | Low-Slack Water | 315.16 | 3.22 | 2.93 | Nan | Nan | Nan |
| 6/21/ 2011 | Low-Slack Water | 35.93 | 5.17 | 4.56 | 12.110 09174 | 2.646 | 4.558 |
| | Flooding | 152.2 | 2.65 | 2.935 | 124.02 95085 | 5.168 | 6.7915 |
| | High-Slack Water | 103.33 | 5.17 | 9.71 | 39.371 62485 | 2.214 | 2.935 |
| 6/27/ 2011 | High-Slack Water | 61.95 | 3.95 | 2.94 | 62.646 06281 | 1.758 | 2.935 |
| | Ebbing | 131.57 | 5.17 | 4.56 | 27.828 72927 | 2.646 | 4.558 |
| | Low-Slack Water | 56.73 | 5.17 | 6.07 | NaN | Nan | Nan |
| 7/6/ 2011 | Low-Slack Water | 59.58 | 1.04 | 2.94 | NaN | Nan | Nan |
| | Flooding | 195.65 | 3.46 | 4.56 | 186.43 88523 | 5.79 | 2.935 |
| | High-Slack Water | 69.35 | 8.92 | 9.71 | 40.063 51096 | 6.345 | 6.7915 |

Table A1: Summary of suspended-sediment observations for June/July 2011.

## Appendix B

## November 2009

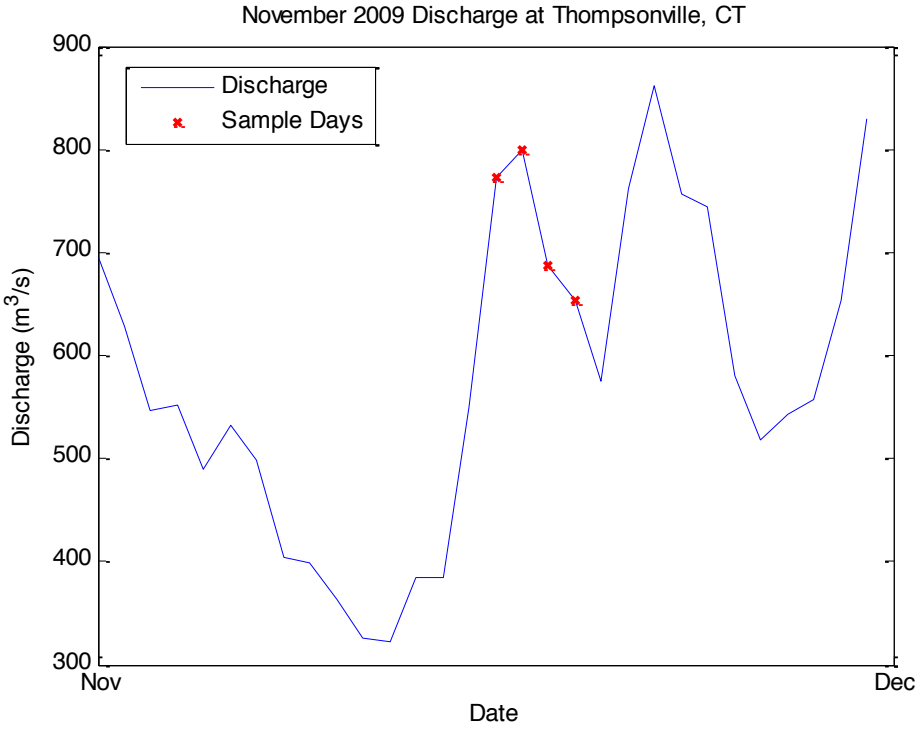


Figure B1: Discharge during the November 2009 study period. Discharge was measured at the USGS gage station on the Connecticut River at Thompsonville, CT.

| Date | Phase of Tide | Max SSC (mg/L) | Position of TM (km) | Position of Max Front (km) |
|---|---|---|---|---|
| 11/16/2009 | Ebbing | 90.69934412 | 5.2344 | 5.1852 |
| | Ebbing | 316.0035063 | 4.9045 | 4.9043 |
| 11/18/2009 | NaN | NaN | NaN | NaN |
| 11/17/2009 | Ebbing | 46.40893997 | 4.4803 | 4.8872 |
| | Ebbing | 84.52716775 | 5.2362 | 5.2964 |
| | Ebbing | 51.73639268 | 5.2713 | 5.2607 |
| | Ebbing | 89.04794744 | 5.2182 | 5.2147 |
| | Ebbing | 79.74327771 | 5.2524 | 5.2321 |
| | Ebbing | 88.00585782 | 5.2378 | 5.253 |
| | Ebbing | 69.62211962 | 5.2748 | 5.2667 |
| 11/19/2009 | Ebbing | 38.57607415 | 6.1824 | 5.9818 |
| | Ebbing | 46.48781262 | 4.696 | 4.4967 |
| | Ebbing | 43.49356918 | 4.9615 | 5.2703 |
| | Ebbing | 77.86799372 | 5.0918 | 5.2193 |
| | Ebbing | 19.83554259 | 5.0599 | 4.9481 |
| | Ebbing | 82.59208316 | 6.4178 | 5.4042 |
| | Ebbing | 110.1062087 | 5.0482 | 5.2069 |
| | Ebbing | 227.6376539 | 5.0428 | 5.016 |
| | Ebbing | 92.38113717 | 5.1821 | 5.2263 |

Table B1: Summary of suspended-sediment observations for November 2009

## Appendix C

## November 2008

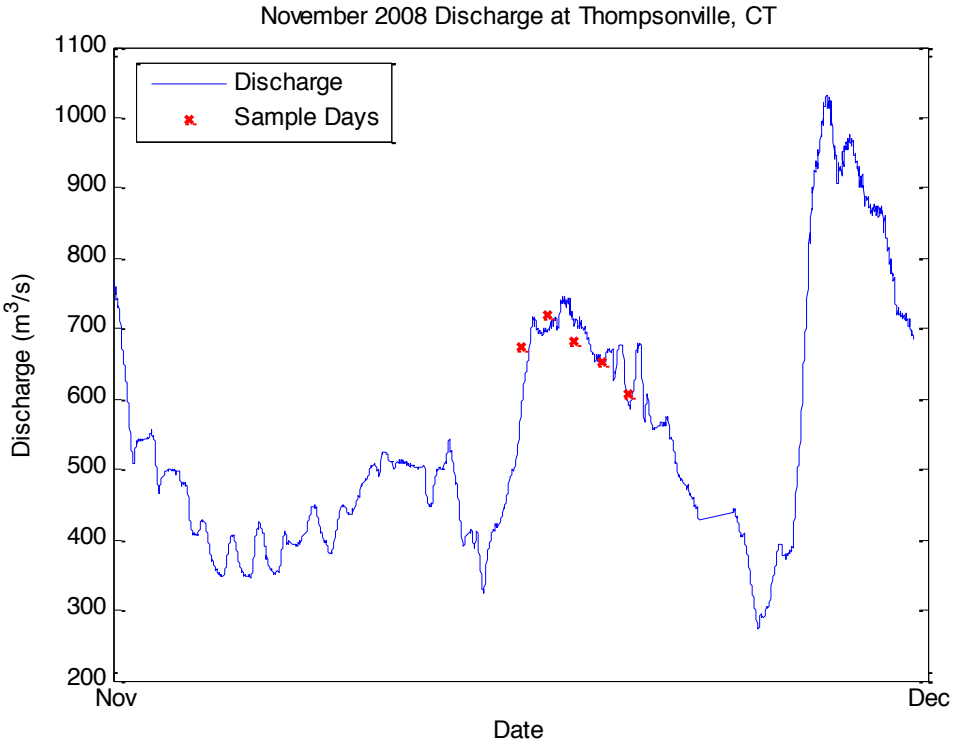


Figure C1: Discharge during the November 2008 study period. Discharge was measured at the USGS gage station on the Connecticut River at Thompsonville, CT.

| Date | Phase of Tide | Max SSC (mg/L) | Position of TM (km) | Position of Max Front (km) | STM (mg/L) | Position of STM (km) | Position of Secondary Front (km) |
|---|---|---|---|---|---|---|---|
| 11/16/ 2008 | ebbing | 181.35 | 9.47 | 7.85 | 47.90 | 7.99 | 8.88 |
| | ebbing | 100.13 | 8.01 | 3.56 | 50.29 | 2.86 | 6.22 |
| | ebbing | 191.56 | 5.67 | 5.03 | 102.47 | 3.47 | 3.21 |
| | ebbing - almost slack | 162.71 | 2.10 | 2.52 | 153.99 | 2.10 | 3.72 |
| 11/17/ 2008 | flooding | 454.08 | 5.44 | 5.42 | 307.92 | 3.35 | 4.19 |
| | flooding | 171.12 | 5.44 | 6.60 | 160.92 | 6.40 | 4.26 |
| | flooding | 192.47 | 8.19 | 8.11 | 114.86 | 6.89 | 7.16 |
| | flooding | 248.55 | 9.50 | 9.10 | 83.96 | 2.93 | 3.72 |
| | High-Slack Water | 46.32 | 9.92 | 9.99 | NaN | NaN | NaN |
| 11/18/ 2008 | flooding | 194.47 | 3.36 | 5.46 | 134.39 | 4.27 | 3.60 |
| | flooding | 91.49 | 4.83 | 7.03 | 61.98 | 6.45 | 3.28 |
| | flooding | 76.98 | 7.23 | 7.99 | 47.99 | 7.23 | 5.58 |
| | flooding | 215.44 | 7.61 | 7.00 | NaN | NaN | NaN |
| | flooding | 59.20 | 8.16 | 9.67 | NaN | NaN | NaN |
| | flooding | 42.12 | 6.81 | 6.85 | NaN | NaN | NaN |
| | High-Slack Water | 43.51 | 7.03 | 10.25 | NaN | NaN | NaN |
| | High-Slack Water | 18.04 | 6.66 | 7.91 | NaN | NaN | NaN |
| | ebbing | 50.51 | 8.01 | 7.92 | NaN | NaN | NaN |
| | ebbing | 16.35 | 7.60 | 7.92 | NaN | NaN | NaN |
| | ebbing | 28.30 | 6.66 | 7.90 | NaN | NaN | NaN |
| | ebbing | 44.72 | 7.60 | 6.73 | NaN | NaN | NaN |
| | ebbing | 72.02 | 7.22 | 6.73 | NaN | NaN | NaN |
| 11/19/ 2008 | flooding | 12.38 | 6.56 | 6.52 | NaN | NaN | NaN |
| | flooding | 264.07 | 2.81 | 7.92 | NaN | NaN | NaN |
| | flooding | 60.33 | 6.53 | 6.55 | NaN | NaN | NaN |
| | flooding | 90.51 | 6.92 | 6.52 | NaN | NaN | NaN |
| | flooding | 139.18 | 6.57 | 7.98 | NaN | NaN | NaN |
| | flooding | 64.78 | 6.90 | 9.11 | NaN | NaN | NaN |
| | flooding | 84.06 | 9.29 | 9.57 | NaN | NaN | NaN |
| | High-Slack Water | 29.42 | 7.08 | 8.09 | NaN | NaN | NaN |
| | ebbing | 18.90 | 7.06 | 6.61 | NaN | NaN | NaN |
| | ebbing | 16.04 | 7.07 | 7.90 | NaN | NaN | NaN |
| | ebbing | 42.81 | 6.55 | 6.56 | NaN | NaN | NaN |
| | ebbing | 25.08 | 6.90 | 7.51 | NaN | NaN | NaN |

Table C1: Summary table of suspended-sediment observations for November 2008.

| | | | | | | | |
|---|---|---|---|---|---|---|---|
| 11/20/2008 | flooding | 87.45 | 0.84 | 3.44 | 66.83 | 2.02 | 1.77 |
| | flooding | 168.96 | 1.52 | 4.43 | 92.08 | 2.05 | 3.43 |
| | flooding | 178.79 | 2.63 | 5.08 | 83.78 | 3.64 | 2.33 |
| | flooding | 112.38 | 2.06 | 5.44 | 76.36 | 5.17 | 3.56 |
| | flooding | 53.87 | 5.69 | 5.78 | NaN | NaN | NaN |
| | flooding | 92.49 | 5.65 | 6.38 | NaN | NaN | NaN |
| | flooding | 44.93 | 5.17 | 7.16 | NaN | NaN | NaN |
| | flooding | 45.10 | 7.09 | 7.72 | NaN | NaN | NaN |
| | flooding | 72.48 | 6.91 | 8.09 | NaN | NaN | NaN |
| | flooding | 42.12 | 7.23 | 8.69 | NaN | NaN | NaN |
| | ebbing | 9.49 | 6.68 | 7.90 | NaN | NaN | NaN |
| | ebbing | 18.27 | 8.00 | 7.91 | NaN | NaN | NaN |
| | ebbing | 11.01 | 6.90 | 7.91 | NaN | NaN | NaN |
| | ebbing | 11.07 | 6.89 | 7.91 | NaN | NaN | NaN |
| | ebbing | 27.19 | 7.23 | 6.50 | NaN | NaN | NaN |
| | ebbing | 36.19 | 6.80 | 6.74 | NaN | NaN | NaN |

Table C1 continued.